

Accepted Manuscript

N-Thiazolylamide-based free fatty-acid 2 receptor agonists: Discovery, lead optimization and demonstration of off-target effect in a diabetes model

Hamid R. Hoveyda, Graeme L. Fraser, Ludivine Zoute, Guillaume Dutheuil, Didier Schils, Cyrille Brantis, Alexey Lapin, Julien Parcq, Sandra Guitard, François Lenoir, Mohamed El Bousmaqui, Sarah Rorive, Sandrine Hospied, Sébastien Blanc, Jérôme Bernard, Frédéric Ooms, Joanne C. McNelis, Jerrold M. Olefsky

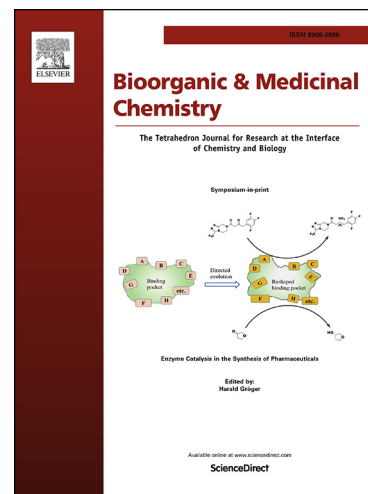
PII: S0968-0896(18)30110-X
DOI: <https://doi.org/10.1016/j.bmc.2018.09.015>
Reference: BMC 14540

To appear in: *Bioorganic & Medicinal Chemistry*

Received Date: 18 January 2018
Revised Date: 13 September 2018
Accepted Date: 16 September 2018

Please cite this article as: Hoveyda, H.R., Fraser, G.L., Zoute, L., Dutheuil, G., Schils, D., Brantis, C., Lapin, A., Parcq, J., Guitard, S., Lenoir, F., Bousmaqui, M.E., Rorive, S., Hospied, S., Blanc, S., Bernard, J., Ooms, F., McNelis, J.C., Olefsky, J.M., *N*-Thiazolylamide-based free fatty-acid 2 receptor agonists: Discovery, lead optimization and demonstration of off-target effect in a diabetes model, *Bioorganic & Medicinal Chemistry* (2018), doi: <https://doi.org/10.1016/j.bmc.2018.09.015>

This is a PDF file of an unedited manuscript that has been accepted for publication. As a service to our customers we are providing this early version of the manuscript. The manuscript will undergo copyediting, typesetting, and review of the resulting proof before it is published in its final form. Please note that during the production process errors may be discovered which could affect the content, and all legal disclaimers that apply to the journal pertain.



N-Thiazolylamide-based free fatty-acid 2
receptor agonists: Discovery, lead optimization
and demonstration of off-target effect in a
diabetes model

*Hamid R. Hoveyda,*¹ Graeme L. Fraser,¹ Ludivine Zoute,¹ Guillaume Dutheil,¹ Didier Schils,^{1, †} Cyrille Brantis,^{1, ■} Alexey Lapin,¹ Julien Parcq,¹ Sandra Guitard,¹ François Lenoir,¹ Mohamed El Bousmaqui,¹ Sarah Rorive,¹ Sandrine Hospied,¹ Sébastien Blanc,¹ Jérôme Bernard,^{1, □} Frédéric Ooms,^{1, ‡} Joanne C. McNelis,² Jerrold M. Olefsky²*

¹Ogeda SA (formerly Euroscreen), 47, rue Adrienne Bolland, 6041 Gosselies, Belgium

²University of California, Department of Medicine, San Diego, CA 92161, USA

Keywords: FFA2 agonist, GPR43 agonist, GPCR, OGTT, LLE, Fsp³

RECEIVED DATE

Abstract:

Free fatty acid-2 (FFA2) receptor is a G-protein coupled receptor of interest in the development of therapeutics in metabolic and inflammatory disease areas. The discovery and optimization of an *N*-thiazolylamide carboxylic acid FFA2 agonist scaffold is described. Dual key objectives were to i) evaluate the potential of this scaffold for lead optimization in particular with respect to safety de-risking physicochemical properties, i.e. lipophilicity and aromatic content, and ii) to demonstrate the utility of selected lead analogues from this scaffold in a pertinent in vivo model such as oral glucose tolerance test (OGTT). As such, a concomitant improvement in bioactivity together with lipophilic ligand efficiency (LLE) and fraction sp³ content (Fsp³) parameters guided these efforts. Compound **10** was advanced into studies in mice on the basis of its optimized profile vs initial lead **1** (Δ LLE = 0.3, Δ Fsp³ = 0.24). Although active in OGTT, **10** also displayed similar activity in the FFA2-knockout mice. Given this off-target OGTT effect, we discontinued development of this FFA2 agonist scaffold.

1. Introduction

We have had a longstanding interest in free fatty acid-2 (FFA2) receptor (previously called GPR43 receptor) as a potential GPCR target towards discovery of novel therapeutics. In 2003, our colleagues¹ as well as Brown and co-workers² reported on the deorphanization of FFA2 receptor and on the role of short chain fatty acids (SCFAs),

consisting of 1-6 carbon atoms, such as acetate and propionate, as potent and selective endogenous agonists to FFA2. Our subsequent efforts culminated in the discovery of several agonist series (e.g. **1**, Figure 1)³ as well as an antagonist⁴ to FFA2 receptor (**2**) thus far mainly documented in our patent filings. These disclosures have in turn fueled recent activities by several groups reporting on their findings with our lead structures⁵ as well as its widespread citation as FFA2 agonist reference ligands.⁶

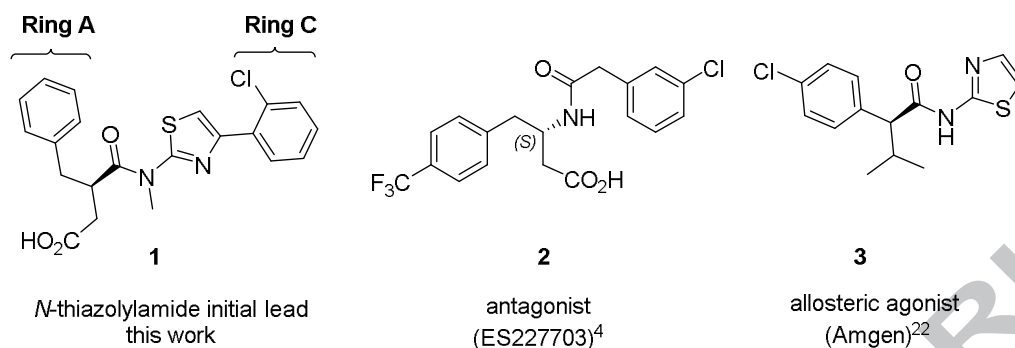
FFA2 receptor is a member of the class A GPCR sub-family that also includes FFA1 (GPR40) and FFA3 (GPR41) receptors, which share 30-40% sequence identity and display specificity toward free fatty acids (FFAs) of various chain lengths.⁵ The FFA2 receptor is expressed in adipose tissue and primary adipocytes and is reported to have a role in promoting adipogenesis through increasing lipid accumulation and inhibiting lipolysis.⁷ In addition, FFA2 receptor is also present in enteroendocrine L-cells,⁸ wherein it mediates GLP-1 release, as well as being expressed in pancreatic islets (β -cells).⁹ Despite the expression of FFA2 in tissues related to lipolysis and glucose metabolism, it is notable that phenotyping studies in FFA2^{-/-} mice have yielded contradictory findings with some reports suggesting that a FFA2 antagonist would be the desired mode of action^{10,11} whereas other studies indicating that an agonist would be required.^{8,12,13,14,15} As there are several examples of FFA2^{-/-} mice displaying phenotypic differences in glucose tolerance,^{8,12,13,14} the oral glucose tolerance test ('OGTT') was used as a measure of in vivo compound efficacy in the current work.

FFA2 receptor is also highly expressed in immune cells such as peripheral blood mononuclear cells (PBMC) and polymorphnuclear cells (PMN) with a particularly high

expression in the neutrophils.¹² In FFA2 receptor knockout mice results in acute colitis studies have reported conflicting results with both reduced¹⁶ and heightened inflammatory responses.¹⁷ More recently, however, seminal studies reported by Garrett and co-workers have helped clarify a role for FFA2 receptor activation in terms of regulation of the colonic T_{reg} pool and protection against colitis.¹⁸ The findings by Garrett et al. combined with the recent lack of success of a FFA2 receptor antagonist in the clinic¹⁹ tend to suggest that agonism of FFA2 receptor is perhaps the relevant mode of action for the treatment of inflammatory disorders.

Some years ago we initiated a screening of carboxylic acid focused libraries using GTP- $\gamma^{35}\text{S}$ assay against *h*FFA2 receptor. Initially these efforts resulted in the discovery of the *N*-thiazolylamide-based carboxylic acid agonist series as well as a potent antagonist to FFA2 receptor (Fig 1). Importantly, antagonist **2** proved a valuable tool in our investigations as it is a potent competitive inhibitor of propionate, the most potent endogenous ligand to FFA2 receptor.²⁰ Consequently, the [³H]-labeled form of **2** (ES227703)²¹ was used in radioligand binding studies where it is displaced by the foregoing *N*-thiazolylamide agonists, but not by the previously identified Amgen allosteric agonist **3**.^{22,23}

The global objectives for the work described herein were to demonstrate the development potential of our *N*-thiazolylamide carboxylic acid FFA2 scaffold in terms of i) lead optimization of key physicochemical properties that impact drug safety (i.e., lipophilicity and aromatic content), and ii) validation of the utility of this scaffold in the metabolic axis using OGTT assay, for which a FFA2^{-/-} mouse model exists. Our results and conclusions with respect to these objectives are summarized below.

Figure 1. Reference ligands herein (nomenclature for SAR discussions indicated).

2. Results and discussion

2.1. Lead optimization strategy

Improving biological activity in parallel to the optimization of physicochemical and pharmacokinetics (PK) properties is a sound approach in modern drug discovery. Property optimization integrated early in the discovery process can help reduce overall early phase attrition due to inadequate safety and/or PK profiles.²⁴ Our lead optimization followed the same guidelines and aimed to concurrently improve the bioactivity (vs *h*FFA2 receptor) as well as the physicochemical properties of the lead structures. Ligand lipophilic efficiency²⁵ ($LLE = pEC_{50} - \log D_{7.4}$)²⁶ and fraction sp^3 ($Fsp^3 = \text{number of } sp^3 \text{ hybridized carbons} / \text{total carbon count}$)²⁷ were principally used to track optimization of properties at this stage of lead optimization. It is well recognized that increased lipophilicity²⁸ and high aromatic content (structural flatness)²⁹ correlate with increased safety risks that lead to greater lead attrition and failure to reach the clinic. It has also been noted that ligands for different target families can be categorized on the basis of the physicochemical property range.³⁰ Overall, we aimed for improved bioactivity combined with $\Delta LLE > 0$ and $\Delta Fsp^3 > 0$ versus the initial lead **1** ($LLE > 4.7$ and $Fsp^3 > 0.19$) in our lead progression efforts not only to

obtain a proof-of-concept (POC) lead to validate the underlying pharmacology, but also to evaluate the potential of this agonist scaffold for physicochemical properties optimization relevant to toxicity de-risking strategy.

2.2. *In vitro* bioactivity SAR

In vitro bioactivity was tracked primarily using GTP- $\gamma^{35}\text{S}$ against *h*FFA2 receptor in Chinese hamster ovary (CHO) cells. GPCR activation by an agonist would ultimately result in the incorporation of GTP- $\gamma^{35}\text{S}$ (guanosine 5'-O-[gamma-thio]triphosphate) that cannot be cleaved to continue the GTP to GDP exchange cycle. Thus, accumulation of GTP- $\gamma^{35}\text{S}$ provides a measure of agonist activity and can be used to derive agonist potency through EC_{50} and $\%E_{\text{max}}$ values at both human and murine orthologues of FFA2 receptor. The GTP- $\gamma^{35}\text{S}$ assay on *h*FFA2 was established using propionate as a reference agonist²⁰ to which our synthetic agonists were relatively compared. Investigation of ligand-receptor affinity with the more active structures was achieved through radioligand binding (RLB) assay using displacement of [^3H]-**2** from recombinant *h*FFA2 receptor in CHO cells.²¹ Since **2** is only active against *h*FFA2 receptor and not against the murine orthologue, the RLB data are available merely against *h*FFA2 receptor (Table 1).³¹ Linear regression analysis for the GTP- $\gamma^{35}\text{S}$ versus the RLB assay displayed a good fit with $r^2 = 0.70$. The GTP- $\gamma^{35}\text{S}$ (pEC_{50} , $\%E_{\text{max}}$) and RLB (pK_i) data were obtained on each compound at least in triplicate with standard deviation $\bullet 0.3$ (Table 1).

As stated above, GTP- $\gamma^{35}\text{S}$ data against *h*FFA2 receptor was the primary SAR driver. Overall, the lead structures herein (**1**, **4-13** in Table 1) were 0.1–0.9 log right-shifted in

comparing human vs murine FFA2 receptor bioactivity data (pEC_{50} , GTP- $\gamma^{35}S$). Chiral SAR was evident since **4**, the chiral antipode to **1**, displayed a 0.5-log right-shift in the GTP- $\gamma^{35}S$ assay and was inactive in the RLB assay. Ester or carboxamide congeners of **1** proved inactive in both assays (data not shown) to thereby establish the indispensability of the carboxylic acid moiety consistent with the findings of previous reports.³²

For brevity, shorthand “Ring A” and “Ring C” notations are used for SAR discussions herein (defined in Figure 1). Aromatic content reduction, or Fsp^3 increase, was feasible through Ring A modifications. For example, cyclopentyl Ring A analogue **5** displayed 0.5-log and 0.2-log improved bioactivity in both GTP- $\gamma^{35}S$ and RLB assays against *h*FFA2 and *m*FFA2 (Table 1), respectively, when compared against its phenyl Ring A congener **1** ($\Delta Fsp^3 = 0.26$). However, LLE remained essentially unchanged in this analogy since the gain in bioactivity (**5** vs **1**: $\Delta pEC_{50, hFFA2} = 0.5$) was essentially nullified by a comparable gain in lipophilicity in the phenyl to cyclopentyl replacement ($\Delta \log D_{7.4} = 0.6$). An attempt to remedy this by introducing polar heteroatoms, e.g. cyclopentyl to tetrahydropyran modification, was unsuccessful due to abrogated bioactivity (**6** vs **5**: $\Delta pEC_{50, hFFA2} = -0.8$, $\Delta pEC_{50, mFFA2} = -1$). In contrast, amide nitrogen substitution provided a means of improving bioactivity and LLE. For instance, converting the *N*-methyl amide in **1** to the corresponding *N*-cyclopropyl amide congener **7** resulted in 0.5-log and 0.2-log improved bioactivity against *h*FFA2 and *m*FFA2, respectively, without an adverse lipophilicity effect ($\Delta \log D_{7.4} = 0$). The *N*-cyclopropyl amide moiety was retained for further rounds of lead optimization (**7-13**, Table 1) due to its appreciable impact on bioactivity and the early-

stage goal of achieving efficacy in the OGTT assay for pharmacology validation of this agonist series.

In contrast to the permissive SAR in the Ring A region of the lead structure, the SAR in the Ring C region was more restrictive, for instance, cycloalkyl or heteroaryl ring replacement of 2-chlorophenyl (**1**, Figure 1) abolished bioactivity altogether (data not shown). An initial notable observation in Ring C SAR was that 2,5-dichloro substitution on the phenyl Ring C (**8**) was more active by 0.4-log and 0.5-log against *h*FFA2 and *m*FFA2, respectively, versus its 2-chlorophenyl congener **7**. However this enhanced activity came at the expense of increased lipophilicity (**7** vs **8**: $\Delta\log D_{7.4} = +0.7$) and consequently the more active lead **8** proved inferior in LLE to **7** by 0.2-0.3 log units (Table 1). As such, we viewed compound **8** as a prototype early generation lead and sought to use the 2,5-substitution pattern on the phenyl Ring C to achieve, as much as possible, concomitant improvement in bioactivity and physicochemical properties.³³ After an extensive systematic investigation, we discovered that replacement of either of the 2- or 5-chloro substituents in Ring C with a heteroaryl ring was well tolerated. Therefore, we reasoned that this substitution strategy is potentially useful towards advanced leads with a more balanced bioactivity and LLE, F_{sp^3} profiles. For example, the analogy between lead structures **9** vs **8** revealed the possibility of achieving the same enhanced bioactivity but with an improved lipophilicity (**9** vs **8**: $\Delta\log D_{7.4} = -0.5$) as reflected by a 0.5-log improved LLE, notwithstanding that both Ring C and Ring A modifications were used to achieve the said results. Ultimately, however, we concluded that the synthetic complexity of the 5-chloro-2-(6-methoxypyridin-3-yl)phenyl Ring C construct exemplified through analogue **9** combined with the added lipophilicity due to 5-chloro substitution outweighed the

improved activity. Therefore, we dropped the 5-chloro moiety in the Ring C construct in **9** in favor of the simpler 2-(6-methoxypyridin-3-yl)phenyl variant and restored the cyclopentyl Ring A to aid with F_{sp^3} increase, which altogether resulted in lead **10** that proved to be the first POC lead in this series as discussed further below. In further attempts to reduce lipophilicity in the advanced lead structure **10**, we used modifications in both Ring A and Ring C. Replacement of the methoxy moiety in the 2-(6-methoxypyridin-3-yl)phenyl Ring C construct in **10** ($\log D_{7.4} = 2.6$) with a pyrazole ring, i.e. **11** ($\log D_{7.4} = 3.1$) was counterproductive as it led to 0.5-log loss in LLE consistent with the similar gain in lipophilicity. Moreover, converting the cyclopentyl ring in **10** to the corresponding isopropyl congener provided compound **12** that displayed a similar bioactivity, but with an improved LLE ($\Delta LLE = 0.4$ based on *h*FFA2 pEC_{50}). The 11-fold superior plasma unbound fraction in isopropyl analogue **12** versus the more lipophilic cyclopentyl congener **10** ($\Delta \log D_{7.4} = -0.4$) combined with >7.5-fold improved unbound total clearance in the foregoing analogy was also noteworthy. Similar trends were also noted in comparing the cyclopentyl analogue **11** to its congener **13** (see Tables 1 and 2).

2.3. *In vivo* efficacy (OGTT) and verification of mode-of-action in FFA2 knockout mice

The oral glucose tolerance test (OGTT) is a common screen performed in mice to measure compound effects on fasting glucose relevant to drug discovery in the field of diabetes and related metabolic disorders. Moreover, phenotypic differences in the OGTT

assay have been reported from various groups using FFA2 *-/-* mice suggestive of a role of FFA2 in glucose tolerance.^{8,12,13,14} Thus, the OGTT assay was selected as an approach to compare the efficacy of compounds *in vivo*. Selection of compounds for *in vivo* efficacy using the OGTT in mice was predicated on the *in vitro* pharmacology profiling as well as oral *in vivo* exposure profile, in particular the dose-normalized unbound oral exposure in mice (cf. oral AUC₀₋₂₄/dose values in Table 2). Although early generation lead structures such as **1** and **7** had reasonable oral exposure (AUC₀₋₂₄) in mouse, these analogues proved to be OGTT inactive. While various groups have published *in vitro* results using either Amgen's allosteric agonist **3**, or our early generation lead **8** in assays such as glucose-stimulated insulin secretion,¹² lipolysis or GLP-1 release,^{33,34} neither **3** nor **8** have ever been reported to elicit any *in vivo* effects, likely due to their rather limited PK exposure (see Table 2). At this stage of testing, we conjectured that perhaps in order to achieve *in vivo* efficacy, further enhanced bioactivity combined with similar or improved PK exposure *vis-à-vis* lead **1** was required. Our lead optimization strategy had provided several second generation lead structures (e.g. **10**, **12** and **13**) with improved bioactivity vs **1** ($\Delta pEC_{50} = 0.3-0.4$) with similar (**10**) or improved (**12** and **13**) dose-normalized unbound oral exposure in mice vs **1**. To our initial satisfaction, these second generation lead structures, i.e. **9-13** (Table 2), proved active in the OGTT assay.

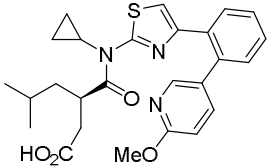
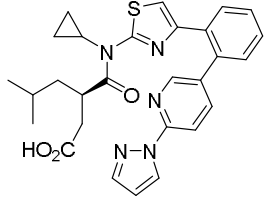
Once *in vivo* compound efficacy was established, a subsequent experiment in wild-type versus FFA2*-/-* mice was carried out with the POC lead **10**, as an OGTT-active lead representative, in order to evaluate the underlying target specificity. As shown in Figure 2, **10** lowered glucose significantly in *both* wild-type *and* in FFA2 receptor knock-out mice *suggesting that the OGTT effect observed is off-target and not FFA2 receptor mediated.*³⁵

It is important to note that **10** proved inactive at 10 μM against alternate FFA receptors (FFA1, FFA3, FFA4) as well as various Type A and Type B GPCRs implicated in metabolic diseases (see Supporting Information for details). Therefore, off-target activity at these related receptors is unlikely to be the cause of the observed OGTT effect and the basis of the OGTT response to **10** remains unexplained. We decided at this stage to discontinue further development of this agonist scaffold based on lack of evidence for FFA2-specific in vivo efficacy.

ACCEPTED MANUSCRIPT

Table 1. Ligand Efficiency Metrics and In Vitro Bioactivity SAR.

Cpd	Structure	logD _{7.4} ^a	Fsp ^{3b}	LLE ^c	GTP-γ ³⁵ S assay ^d		RLB		
					pEC ₅₀	%E _{max}	pK _i		
1	see Fig 1	2.3	0.19		4.7	h	7.0	106	6.1
					4.3	m	6.6	81	-
3	see Fig 1	3.9	0.29		3.1	h	7.0	94	-
					2.9	m	6.8	77	-
4	<i>S</i> -enantiomer of 1	2.3	0.19		4.2	h	6.5	57	< 5
					3.8	m	6.1	69	-
5		2.9	0.45		4.6	h	7.5	84	6.6
					3.9	m	6.8	63	-
6		1.3	0.45		5.4	h	6.7	103	5.7
					4.5	m	5.8	76	-
7		2.3	0.26		5.2	h	7.5	104	6.4
					4.5	m	6.8	86	-
8		3.0	0.26		4.9	h	7.9	125	6.7
					4.3	m	7.3	113	-
9		2.5	0.26		5.4	h	7.9	126	7.0
					4.8	m	7.3	94	-
10		2.6	0.43		5.0	h	7.6	110	6.8
					4.4	m	7.0	81	-
11		3.1	0.37		4.5	h	7.6	108	7.2
					4.0	m	7.1	72	-

12		2.2	0.39	5.4	h	7.6	103	6.6
				4.7	m	6.9	84	-
13		2.4	0.32	5.2	h	7.6	104	6.8
				4.6	m	7.0	88	-

^a LogD measured by HPLC at pH 7.4, $N = 3$ and $\%RSD \bullet 2$ (See Supporting Information for details).²⁶ ^b F_{sp^3} or fraction sp^3 = number of sp^3 hybridized carbons/total carbon count. ^c LLE = $pEC_{50} - \log D_{7.4}$. ^d GTP- $\gamma^{35}S$ assay data for human (*h*) and murine (*m*) orthologues of FFA2 receptor provided. GTP- $\gamma^{35}S$ (pEC_{50} , $\%E_{max}$) and RLB (pK_i) data were obtained on each compound at least in triplicate with standard deviation $\bullet 0.3$.

ACCEPTED MANUSCRIPT

Table 2. Plasma Protein Binding, Pharmacokinetics^a and OGTT Efficacy Profiles.

Cpd	plasma f_u		rat PK (iv 1 mg/kg, oral 3 mg/kg)				mouse PK (50 mg/kg)	OGTT % inhibition (peak) at 50 mg/kg ^b
	rat	mouse	iv CL _u	iv T _{1/2} (min)	%F	oral AUC _u / dose	oral AUC _u /dose	
1	0.0008	0.0015	738	482	77	2.4	2.0	-8 ± 5% (<i>p</i> > 0.05)
3^c	0.0062	0.0052	6666	220	15	0.08	0.045	7 ± 6% (<i>p</i> > 0.05)
7	0.0016	0.0025	1044	319	52	0.70	4.7	1 ± 5% (<i>p</i> > 0.05)
8	0.0001	0.0001	2800	590	47	0.26	0.32	5 ± 5% (<i>p</i> > 0.05)
9	0.0026	0.0041	2738	579	38	0.26	1.2	32 ± 6% (<i>p</i> < 0.001)
10	0.0006	0.0023	2617	240	47	0.29	2.1	33 ± 7% (<i>p</i> < 0.001)
11	0.0013	0.0014	6692	155	25	0.07	0.53	40 ± 4% (<i>p</i> < 0.001)
12	0.0066	0.0107	342	431	35	2.1	4.7	19 ± 5% (<i>p</i> < 0.01)
13	0.0057	0.0075	1091	280	29	0.55	3.3	26 ± 5% (<i>p</i> < 0.001)

^a PK formulation: 1% DMSO, 9% hydroxypropyl- β -cyclodextrin in 0.9% NaCl. Unbound PK parameters calculated as follows: iv CL_u (mL/min/Kg) = CL_{T,iv} / (plasma f_u); AUC_u = AUC_T (in μ M.min) x (plasma f_u).^b OGTT formulation is the same as that for PK studies but without DMSO. Statistical analysis performed by 2-way ANOVA followed by Bonferroni's posthoc analysis directly provided in parenthesis. OGTT % inhibition presented as data \pm SEM. Statistically significant OGTT data highlighted in bold. ^c Tested at 3 mg/kg in mouse PK and 8.4 mg/kg in OGTT due to limited solubility.

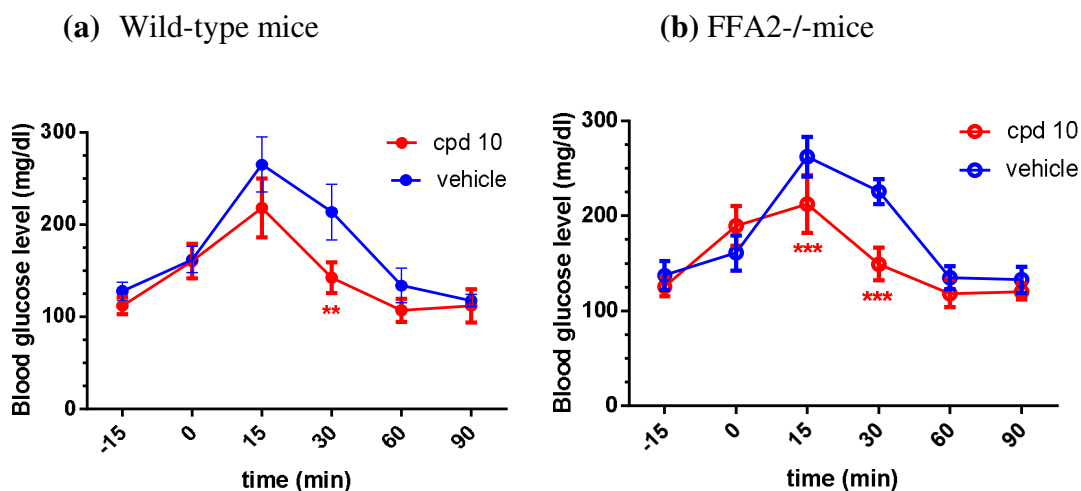


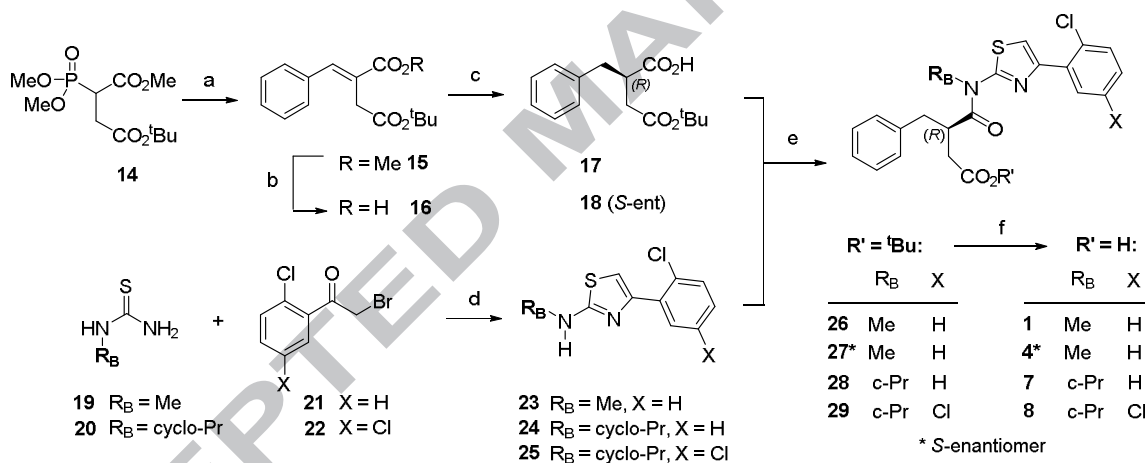
Figure 2. Oral glucose tolerance test (OGTT) assay results with **10** (50 mg/kg) in (a) wild-type and (b) FFA2 receptor knock-out mice.¹² Vehicle: 9% hydroxypropyl- β -cyclodextrin in 0.9% NaCl. The results are shown as mean \pm SEM. Statistical analysis performed by 2-way ANOVA followed by Bonferroni's posthoc analysis: *** $p < 0.001$, ** $p < 0.01$.

2.4. Chemistry

The preparative routes used to access the compounds described in this paper are illustrated in Schemes 1-3. The synthesis of *N*-thiazolylamide-based analogues required access to two key reagents: the Ring A (Figure 1) bearing chiral building block, e.g. **17** (Scheme 1), and the 2-aminothiazole building block bearing Rings B and C, e.g. **23** (Scheme 1). For analogues **1**, **4**, **7** and **8**, the chiral carboxylic acid building block (**17**, **18**) was prepared through Horner-Wadsworth-Emmons synthesis followed by Noyori asymmetric hydrogenation. The chiral acid-ester building blocks for the remaining of lead structures herein (**5-6**, **9-13**) were prepared using the Evans oxazolidinone chiral auxiliary approach (**42-45**, Scheme 2). The 2-aminothiazole building blocks (**23-25**, Scheme 1) were assembled using Hantzsch thiazole synthesis through condensation of substituted thioureas with α -bromoacetophenones. For lead compounds **9-13** (Table 1), the corresponding 2-aminothiazole building blocks **50-53** were prepared by a

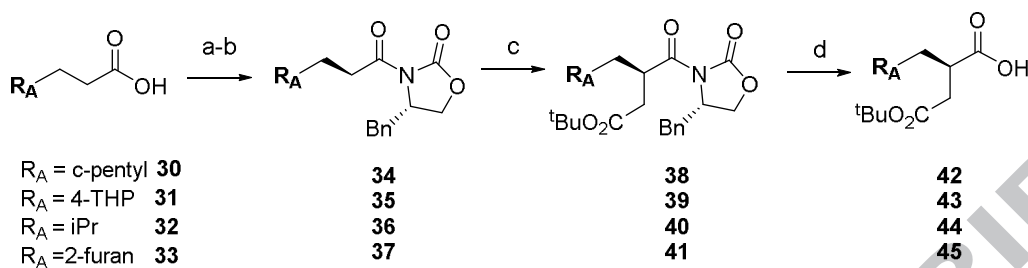
combination of Hantzsch thiazole synthesis and Pd-catalyzed Suzuki cross-coupling (Scheme 3). The final target structure was assembled in ester form through HATU-mediated amide coupling between the chiral carboxylic acid and 2-aminothiazole building blocks at room temperature or at 60 °C with sterically encumbered *N*-cyclopropyl-2-aminothiazoles (**24-25** and **50-53**) to achieve comparable yields.³⁶ Finally, TFA-mediated deprotection of the *tert*-butyl ester moiety afforded the final product in free carboxylic acid form. We favored the use of *tert*-butyl ester precursors since the acidolytic deprotection with TFA was less prone to racemization in contrast to saponification of related methyl ester derivatives in aqueous milieu.

Scheme 1. Synthesis of analogues 1, 4, 7 and 8.^a



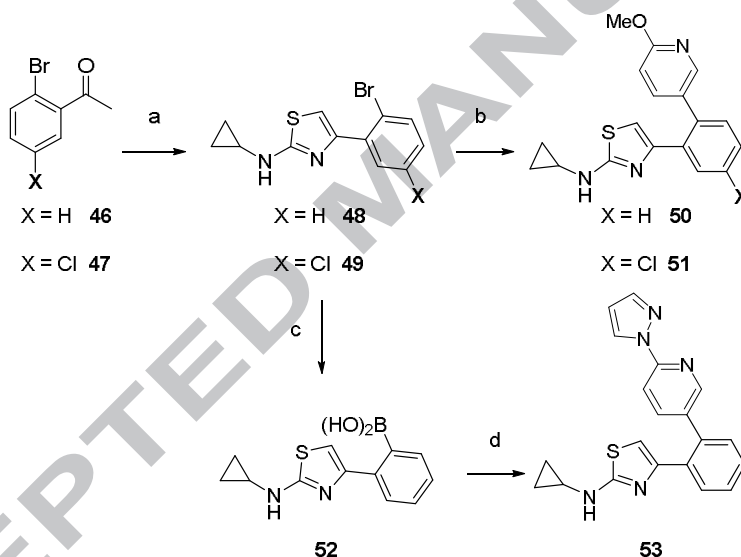
^a Reagents and conditions: (a) *n*BuLi, THF, 5-15 °C then PhCHO, THF, 5-15°C to rt; (b) *n*Bu₄OH (1M in water), THF, rt; (c) dicyclohexylamine, RuCl₂[(*S*)-BINAP], H₂ (8-10 bar), MeOH, 55°C; (d) EtOH, reflux; (e) HATU, DIEA, CH₃CN, rt (with **23**) or 60 °C (with **24** and **25**); (f) TFA, DCM, rt.

Scheme 2. Preparation of chiral acid building blocks via Evans oxazolidinone auxiliary approach to synthesize 5, 6, 9-13.^a



^a Reagents and conditions: (a) TEA, pivaloyl chloride, THF, $-78\text{ }^{\circ}\text{C}$ to rt; (b) nBuLi, (*S*)-4-benzyloxazolidin-2-one, THF, $-78\text{ }^{\circ}\text{C}$; (c) NaHMDS, *tert*-butyl 2-bromoacetate; THF, $-78\text{ }^{\circ}\text{C}$ to rt; (d) $\text{H}_2\text{O}_2/\text{LiOH}$, THF/ H_2O , $0\text{ }^{\circ}\text{C}$ to rt.

Scheme 3. Preparation of *N*-cyclopropyl-4-biaryl-thiazole-2-amine building blocks used to synthesize 9-13.^a



^a Reagents and conditions: (a) (i) AlCl_3 , Br_2 , THF, $0\text{ }^{\circ}\text{C}$ to rt; (ii) 1-cyclopropylthiourea, EtOH, reflux; (b) $\text{ArB}(\text{OH})_2$, K_2CO_3 , *S*-Phos, $\text{Pd}_2(\text{dba})_3$, toluene, $85\text{ }^{\circ}\text{C}$; (c) nBuLi, $\text{B}(\text{O}i\text{-Pr})_3$, THF, $-78\text{ }^{\circ}\text{C}$ to rt; (d) $\text{Pd}(\text{PPh}_3)_4$, ArBr, K_2CO_3 , toluene, $85\text{ }^{\circ}\text{C}$.

3. Conclusion

As stated in the Introduction, we had two global objectives in the work presented herein. The first objective was to verify if the *N*-thiazolylamide carboxylic acid FFA2 agonist scaffold that

we had discovered in our HTS campaigns is amenable to physicochemical properties optimization relevant to safety de-risking strategies. Lipophilicity and aromatic content optimization were thus undertaken and tracked through the use of LLE and Fsp³ metrics to gauge whether these properties lend themselves to improvement against the initial lead **1**. As depicted in Figure 3 in the early round of lead optimization, compound **8** emerged as a lead displaying improved LLE and Fsp³ albeit with the undesirable 0.7-log increase in lipophilicity. For the latter reason, we viewed structure **8** as a prototype towards more balanced lead structures in terms of physicochemical properties relevant to safe drug development. Further lead optimization efforts furnished structures with much improved Fsp³ (**10-13**) and lipophilicity similar to the initial lead **1** (**10, 12-13**). Among these, compound **10** was chosen as the POC lead candidate. Overall, these results indicated that the physicochemical property optimization of this scaffold is feasible, although more limited in terms of lipophilicity improvement than aromatic content.

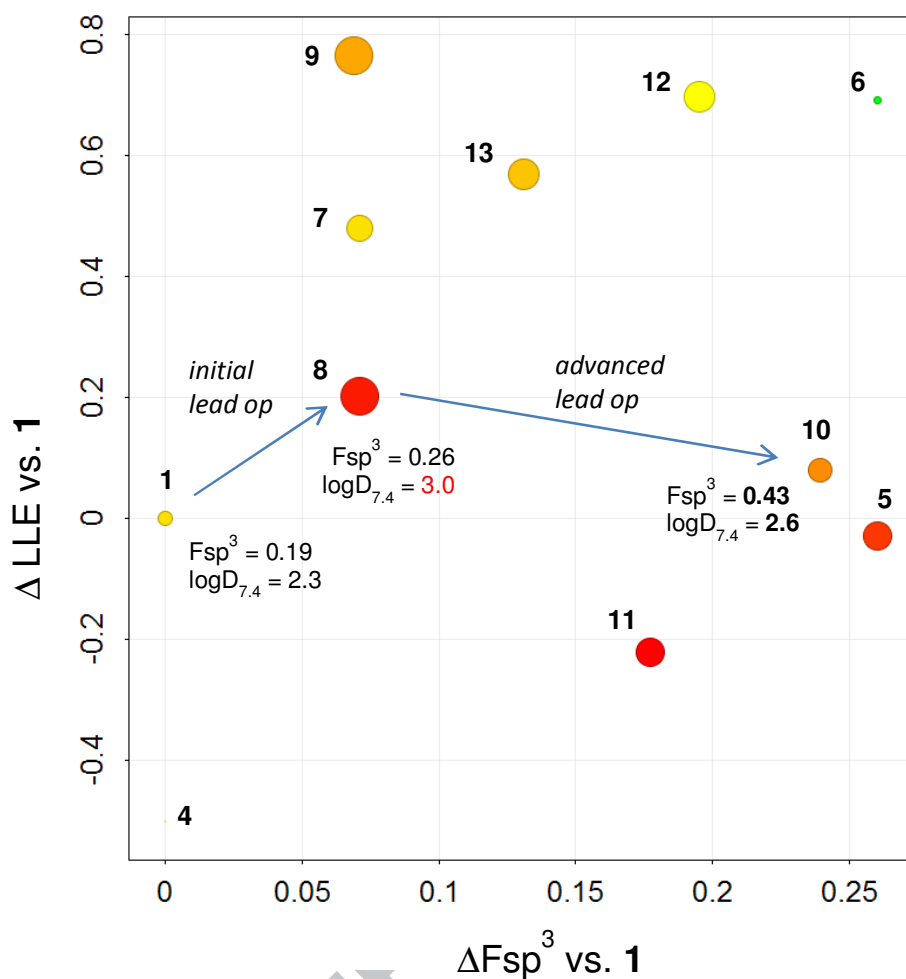


Figure 3. Lead optimization progress as a plot of $\Delta LLE = LLE(\text{cpd } x) - LLE(\text{cpd } 1)$ versus $\Delta F_{sp}^3 = F_{sp}^3(\text{cpd } x) - F_{sp}^3(\text{cpd } 1)$. LLE and F_{sp}^3 as defined in Table 1. Color code: green = low lipophilicity (i.e. $\log D_{7.4}$) and red = high lipophilicity. Size of dots refers to $hFFA2$ pEC_{50} with larger dots reflecting more potent compounds in this bioassay and conversely.

The second key objective in this program was to establish *in vivo* efficacy in an assay such as OGTT that is both relevant to metabolic disease axis and has been validated using $FFA2^{-/-}$ mice by other groups. After ensuring that the test compounds possess adequate oral exposure *in vivo*, a number of lead structures were thus selected and screened in OGTT assay (Table 2). The analogs tested encompassed structures from the foregoing scaffold both from the initial (1, 7 and 8) as well as advanced optimization rounds (10-13). As noted in Table 2, OGTT effect was

observed merely with the advanced leads (i.e. **9-13**) and not with the early lead structures (**1, 7** and **8**). However, in a subsequent step to validate the mechanism of action underlying compound activity, the POC lead **10** was observed to have similar efficacy in both wild-type and FFA2 knockout mice indicating that the OGTT effect is not FFA2 mediated (Fig 2). Irrespective of the underlying cause for this off-target OGTT effect, we decided to terminate this project as we failed to demonstrate specific, FFA2-mediated *in vivo* efficacy. We shall disclose in due course our findings with an alternative proline-based scaffold that can indeed serve as a *bona fide* agonist reference for FFA2 receptor.³⁷

4. Experimental section

4.1 Chemistry

All reactions were performed under a nitrogen atmosphere at rt using anhydrous grade solvents except as otherwise noted. All reagents were used as supplied by the vendor except as noted. Compd **2** was prepared as described elsewhere;⁴ **3** was purchased from Enamine. NMR spectra were recorded on Bruker ARX spectrometer (300 MHz) at rt. Chemical shifts are expressed in parts per million relative to residual solvent as an internal reference. Peak multiplicities are expressed as follows: singlet (s), doublet (d), triplet (t), quartet (q), heptuplet (h), multiplet (m), and broad singlet (bs). HPLC purity analysis was carried out using one of the following methods.

Method A: LC/diode array detector coupled to single quadrupole mass spectrometry (LC/UV/MS); column: Sunfire C18 3 μ m 3.0 \times 50 mm; mobile phase A: 0.1% TFA in water (v/v); mobile phase B: 0.1% TFA in CH₃CN (v/v); gradient begins at 5% B, hold 0.2 min at 5% B, increasing to 95% B over 6.0 min, hold at 95% B until 7.75 min; flow rate: 1.0 mL/min.

Method B: LC/diode array detector coupled to single quadrupole mass spectrometry

(LC/UV/MS); column: Sunfire C18 3 μ m 3.0 \times 50 mm; mobile phase A: 0.1% TFA in water (v/v); mobile phase B: 0.1% TFA in CH₃CN (v/v); gradient begins at 5% B, hold 0.2 min at 5% B, increasing to 95% B over 2.0 min, hold at 95% B until 3.75 min; flow rate: 1.0 mL/min. Enantiomeric excess reported as %ee and determined using one of the following methods. *Method C (chiral)*: column: Chiralpak ID 5.0 μ m C18 4.6 \times 250 mm; mobile phase: 0.1% TFA in hexane/EtOH (95:5 v/v); flow rate: 1.0 mL/min; UV absorbance at 215 nm. *Method D (chiral)*: column: Chiralpak ID 5.0 μ m C18 4.6 \times 250 mm; mobile phase: 0.1% TFA in hexane/*i*-PrOH (99:1 v/v); flow rate: 1.5 mL/min; UV absorbance at 254 nm. *Method E (chiral)*: column: Chiralpak IB 5.0 μ m C18 4.6 \times 250 mm; mobile phase: 0.1% TFA in hexane/*i*-PrOH (98:2 v/v); flow rate: 1.5 mL/min; UV absorbance at 254 nm. *Method F*: column: Chiralpak IC 5.0 μ m C18 4.6 \times 250 mm; mobile phase: 0.1% TFA in hexane/*i*-PrOH (80:20 v/v); flow rate: 1.0 mL/min; UV absorbance at 254 nm. PerkinElmer ChemDraw Ultra software (ver 15) was used for naming the compounds described below.

4.2. (*R*)-3-Benzyl-4-((4-(2-chlorophenyl)thiazol-2-yl)(methyl)amino)-4-oxobutanoic acid (**1**).

Amide Bond Formation Step: To a solution of carboxylic acid **17** (6 g, 22.6 mmol) in CH₃CN (0.4 M) under Ar was added HATU (8.6 g, 22.6 mmol) and the mixture stirred for 10 min whereupon aminothiazole **23** (5.1 g, 22.6 mmol) was added followed by DIEA (4.1 mL, 24.8 mmol) and the mixture stirred typically overnight. The volatiles were then removed in vacuo and the residue thus obtained taken up in DCM (500 mL) and washed with saturated sodium bicarbonate (500 mL). The organic layers were then washed with 1N HCl (500 mL), brine (500 mL), dried over MgSO₄, filtered and concentrated to dryness and the crude thus obtained subjected to silica gel flash chromatography (10% EtOAc in cyclohexane) to obtain pure *tert*-butyl(*R*)-3-benzyl-4-((4-(2-chlorophenyl)thiazol-2-yl)(methyl)amino)-4-oxobutanoate (**26**) as

white solid (10 g, 94%). LCMS (Method B) m/z 471 ($M + 1$). HPLC purity > 98% (254 nm). ^1H NMR (300 MHz, CDCl_3) 7.93 (dd, $J = 1.8, 7.7$ Hz, 1H), 7.53 (s, 1H), 7.44 (dd, $J = 1.2, 7.7$ Hz, 1H), 7.34 - 7.16 (m, 7H), 3.63 (s, 3H), 3.68 - 3.58 (m, 1H), 3.07 - 2.96 (m, 2H), 2.77 (dd, $J = 7.2, 13.4$ Hz, 1H), 2.47 (dd, $J = 4.0, 17.0$ Hz, 1H), 1.36 (s, 9H). *Tert-butyl Ester Deprotection Step:* To a solution of *tert*-butyl ester **26** (10 g, 21.2 mmol) in 250 mL DCM was added TFA (31.7 mL, 0.42 mmol) at rt and the mixture stirred typically for 2-3 h. The mixture was then diluted with EtOAc (1 L) and the organic phase washed thoroughly with 10% sodium bisulfite (500 mL) and brine (500 mL). The extracted organic layer was dried (Na_2SO_4), filtered and concentrated to dryness in vacuo to obtain **1** as white solid (8 g, 92%). LCMS (Method A) m/z 415 ($M + 1$). HPLC purity > 99% (254 nm). Chiral LC (Method D) 98.8 %ee ($t_{R(S)} = 6.2$ min, $t_{R(R)} = 9.0$ min). ^1H NMR (CDCl_3): 7.91 (dd, $J = 1.7, 7.8$ Hz, 1H), 7.54 (s, 1H), 7.45 (dd, $J = 1.2, 7.8$ Hz, 1H), 7.34 - 7.20 (m, 5H), 7.25 - 7.17 (m, 2H), 3.72 - 3.64 (m, 1H), 3.63 (s, 3H), 3.15 - 3.02 (m, 2H), 2.78 (dd, $J = 7.0, 13.9$ Hz, 1H), 2.58 (dd, $J = 2.1, 18.3$ Hz, 1H). ^{13}C NMR (CDCl_3): 177.5, 174.3, 158.6, 145.5, 137.5, 133.5, 132.1, 131.3, 130.6, 129.0, 128.9, 128.7, 127.3, 127.0, 114.7, 41.3, 38.9, 36.4, 34.9. HRMS: calcd 415.0883, found 415.0876, $\text{C}_{21}\text{H}_{20}\text{ClN}_2\text{O}_3\text{S}$. Elemental Analysis: calcd C, 60.79; H, 4.62; N, 6.75; found C, 60.11; H, 4.67; N, 6.49.

4.3. (*S*)-3-Benzyl-4-((4-(2-chlorophenyl)thiazol-2-yl)(methyl)amino)-4-oxobutanoic acid (**4**). As per compd **1** synthesis, amide coupling between acid **18** (77 mg, 0.29 mmol) and aminothiazole **23** (78 mg, 0.35 mmol) furnished *tert*-butyl(*S*)-3-benzyl-4-((4-(2-chlorophenyl)thiazol-2-yl)(methyl)amino)-4-oxobutanoate (**27**) as a white solid (125 mg, 90%) after flash chromatography (15% EtOAc in cyclohexane). LCMS (Method B) m/z 471 ($M + 1$). HPLC purity > 98% (254 nm). ^1H NMR (300 MHz, CDCl_3) as above. **27** (125 mg, 0.26 mmol) after

TFA deprotection, as per compd **1**, afforded **4** as white solid (85 mg, 79%). LCMS (Method A) m/z 415 ($M + 1$). HPLC purity: 98% (254 nm). Chiral LC (Method D) 84.2 %ee ($t_{R(S)} = 6.2$ min, $t_{R(R)} = 9.0$ min). Preparative chiral LC purification was performed to afford **4** with HPLC purity > 99% (254 nm) and chiral LC (Method D) > 99 %ee $^1\text{H NMR}$ (CDCl_3): 7.91 (dd, $J = 1.7, 7.8$ Hz, 1H), 7.54 (s, 1H), 7.45 (dd, $J = 1.2, 7.8$ Hz, 1H), 7.34 – 7.20 (m, 5H), 7.23 – 7.15 (m, 2H), 3.71 – 3.65 (m, 1H), 3.63 (s, 3H), 3.15 – 3.02 (m, 2H), 2.78 (dd, $J = 7.0, 13.9$ Hz, 1H), 2.58 (dd, $J = 2.1, 18.3$ Hz, 1H). $^{13}\text{C-NMR}$ (CDCl_3): 177.5, 174.3, 158.6, 145.5, 137.5, 133.5, 132.1, 131.3, 130.6, 129.0, 128.9, 128.7, 127.3, 127.0, 114.7, 41.3, 38.9, 36.4, 34.9. HRMS: calcd 415.0883, found 415.0891, $\text{C}_{21}\text{H}_{20}\text{ClN}_2\text{O}_3\text{S}$.

4.4. (*R*)-4-((4-(2-Chlorophenyl)thiazol-2-yl)(methyl)amino)-3-(cyclopentylmethyl)-4-oxo butanoic acid (**5**). As per compd **1** synthesis, amide coupling between acid **42** (50 mg, 0.20 mmol) and aminothiazole **23** (44 mg, 0.20 mmol) furnished *tert*-butyl (*R*)-4-((4-(2-chlorophenyl)thiazol-2-yl)(methyl)amino)-3-(cyclopentylmethyl)-4-oxobutanoate (**54**) as white solid (56 mg, 62%) after flash chromatography (2-20% EtOAc in cyclohexane). LCMS (Method B) m/z 464 ($M + 1$). HPLC purity > 98% (254 nm). **54** (58 mg, 0.13 mmol) after TFA deprotection, as per compd **1**, afforded **5** as white solid (20 mg, 39%). LCMS (Method A) m/z 407 ($M + 1$). HPLC purity > 99% (254 nm). Chiral LC (Method D) 99.4 %ee ($t_{R(R)} = 5.2$ min, $t_{R(S)} = 10.2$ min). $^1\text{H NMR}$ (CDCl_3): 7.96 (dd, $J = 1.5, 7.7$ Hz, 1H), 7.54 (s, 1H), 7.46 (dd, $J = 1.3, 7.7$ Hz, 1H), 7.33 (dt, $J = 1.3, 7.7$ Hz, 1H), 7.25 (dt, $J = 1.5, 7.7$ Hz, 1H), 3.92 (s, 3H), 3.46 - 3.42 (m, 1H), 3.04 (dd, $J = 9.9, 17.4$ Hz, 1H), 2.63 (dd, $J = 4.0, 7.5$ Hz, 1H), 1.83 – 1.68 (m, 4H), 1.64 – 1.46 (m, 6H), 1.18 – 1.04 (m, 2 H). $^{13}\text{C NMR}$ (CD_3OD): 177.6, 178.6, 160.3, 146.8, 134.9, 133.1, 132.5, 131.5, 130.0, 125.0, 115.5, 40.1, 39.7, 38.9, 37.8, 35.8, 34.2, 33.7, 26.1, 26.0. HRMS: calcd 407.1196, found 407.1191, $\text{C}_{20}\text{H}_{24}\text{ClN}_2\text{O}_3\text{S}$.

4.5. (*R*)-4-((4-(2-Chlorophenyl)thiazol-2-yl)(methyl)amino)-4-oxo-3-((tetrahydro-2*H*-pyran-4-yl)methyl)butanoic acid (**6**). As per compd **1** synthesis, amide coupling between acid **43** (50 mg, 0.18 mmol) and **23** (45 mg, 0.20 mmol) furnished *tert*-butyl (*R*)-4-((4-(2-chlorophenyl)thiazol-2-yl)(methyl)amino)-4-oxo-3-((tetrahydro-2*H*-pyran-4-yl)methyl)butanoate (**55**) as white solid (77 mg, 89%) after flash chromatography (20% EtOAc in cyclohexane). LCMS (Method A) *m/z* 479 (*M* + 1). HPLC purity > 98% (254 nm). **55** (77 mg, 0.16 mmol) after TFA deprotection, as per compd **1**, afforded **6** as white solid (26 mg, 38%). LCMS (Method A) *m/z* 423 (*M* + 1). HPLC purity > 99% (254 nm). Chiral LC (Method E) 99.3 %ee (*t_{R(R)}* = 6.4 min, *t_{R(S)}* = 9.3 min). ¹H-NMR (CDCl₃): 7.95 (dd, *J* = 1.5, 7.5 Hz, 1H), 7.54 (s, 1H), 7.46 (dd, *J* = 1.2, 7.8 Hz, 1H), 7.33 (dt, *J* = 1.2, 7.5 Hz, 1H), 7.28 – 7.23 (m, 1H), 3.99 – 3.92 (m, 2H), 3.90 (s, 3H), 3.54 – 3.47 (m, 1H), 3.39 – 3.32 (m, 2H), 3.01 (dd, *J* = 9.5, 17.4 Hz, 1H), 2.59 (dd, *J* = 4.0, 7.3 Hz, 1H), 1.71 – 1.48 (m, 5H), 1.39 – 1.20 (m, 3H). ¹³C-NMR (CDCl₃): 176.4, 174.9, 158.8, 145.6, 133.5, 132.1, 131.3, 130.7, 128.8, 127.0, 114.8, 67.8, 67.7, 39.4, 38.5, 36.2, 36.0, 35.1, 33.6, 32.9, 32.6, 32.5, 32.2. HRMS: calcd 423.1145, found 423.1151, C₂₀H₂₄ClN₂O₄S.

4.6. (*R*)-3-Benzyl-4-((4-(2-chlorophenyl)thiazol-2-yl)(cyclopropyl)amino)-4-oxobutanoic acid (**7**). Using acid **17** (200 mg, 0.76 mmol) and aminothiazole **24** (190 mg, 0.76 mmol) amide bond formation step was carried out as per compd **1** except at 60 °C to obtain *tert*-butyl (*R*)-3-benzyl-4-((4-(2-chlorophenyl)thiazol-2-yl)(cyclopropyl)amino)-4-oxo butanoate (**28**) as yellow oil (232 mg, 62%) after flash chromatography (10% EtOAc in cyclohexane). LCMS (Method B) *m/z* 497 (*M* + 1). HPLC purity > 98% (254 nm). **28** (170 mg, 0.34 mmol) after TFA deprotection, as per compd **1**, afforded **7** as white solid (120 mg, 71%). LCMS (Method A) *m/z* 441 (*M* + 1). HPLC purity: 94% (254 nm). Chiral LC (Method E) 95.4 %ee (*t_{R(R)}* = 4.5 min, *t_{R(S)}* = 7.1 min). ¹H NMR (CDCl₃): 7.91 (dd, *J* = 1.8, 7.8 Hz, 1H), 7.54 (s, 1H), 7.46 (dd, *J* = 1.3, 7.8

Hz, 1H), 7.34 – 7.14 (m, 7H), 4.19 – 4.11 (m, 1H), 3.09 (dd, $J = 6.2, 13.2$ Hz, 1H), 3.03 – 2.91 (m, 2H), 2.72 (dd, $J = 8.2, 13.2$ Hz, 1H), 2.54 – 2.47 (m, 1H), 1.15 – 1.10 (m, 3H), 0.88 – 0.80 (m, 1H). HRMS: calcd 441.1040, found 441.1048, $C_{23}H_{22}ClN_2O_3S$.

4.7. (*R*)-3-Benzyl-4-(cyclopropyl(4-(2,5-dichlorophenyl)thiazol-2-yl)amino)-4-oxobutanoic acid (**8**). Using acid **17** (100 mg, 0.38 mmol) and aminothiazole **25** (108 mg, 0.38 mmol) amide bond formation step was carried out as per compd **1** except at 60 °C to obtain *tert*-butyl (*R*)-3-benzyl-4-(cyclopropyl(4-(2,5-dichlorophenyl)thiazol-2-yl)amino)-4-oxobutanoate (**29**) as white solid (152 mg, 76%) after flash chromatography (10% EtOAc in cyclohexane). LCMS (Method B) m/z 531 ($M + 1$). HPLC purity > 98% (254 nm). 1H NMR ($CDCl_3$): 7.91 (d, $J = 2.6$ Hz, 1H), 7.55 (s, 1H), 7.31 (d, $J = 8.6$ Hz, 1H), 7.27 – 7.08 (m, 6H), 4.18 – 4.11 (m, 1H), 2.88 – 2.61 (m, 3H), 2.36 (dd, $J = 16.7, 4.9$ Hz, 1H), 1.31 (s, 9H), 1.25 – 1.13 (m, 4H), 0.78 – 0.69 (m, 1H). **29** (152 mg, 0.29 mmol) after TFA deprotection, as per compd **1**, afforded **8** as white solid (82 mg, 60%). LCMS (Method A) m/z 475 ($M + 1$). HPLC purity > 99% (254 nm). 1H NMR ($CDCl_3$): 7.96 (d, $J = 2.3$ Hz, 1H), 7.63 (s, 1H), 7.38 (d, $J = 8.5$ Hz, 1H), 7.28 – 7.18 (m, 4H), 7.18 – 7.10 (m, 2H), 4.21 – 4.15 (m, 1H), 3.14 – 2.86 (m, 3H), 2.73 (dd, $J = 8.5, 13.6$ Hz, 1H), 2.53 (dd, $J = 4.0, 17.4$ Hz, 1H), 1.25 – 1.19 (m, 3H), 0.88 – 0.78 (m, 1H). HRMS: calcd 475.0650, found 475.0649, $C_{23}H_{21}Cl_2N_2O_3S$.

4.8. (*R*)-4-((4-(5-Chloro-2-(6-methoxy pyridin-3-yl)phenyl)thiazol-2-yl)(cyclopropyl)amino)-3-(furan-2-ylmethyl)-4-oxobutanoic acid (**9**). Using acid **45** (100 mg, 0.39 mmol) and aminothiazole **51** (141 mg, 0.44 mmol) amide bond formation step carried out as per compd **1** except at 60 °C to obtain *tert*-butyl (*R*)-4-((4-(5-chloro-2-(6-methoxy pyridin-3-yl)phenyl)thiazol-2-yl)(cyclopropyl)amino)-3-(furan-2-ylmethyl)-4-oxobutanoate (**56**) as a white solid (62 mg, 37%) after flash chromatography (20% EtOAc in cyclohexane). LCMS (Method B) m/z 595 (M

+ 1). HPLC purity > 98% (254 nm). **56** (85 mg, 0.14 mmol, two batches combined) after TFA deprotection, as described for **1**, afforded **9** as white solid (60 mg, 78%). LCMS (Method A) m/z 538 ($M + 1$). HPLC purity 95% (254 nm). ^1H NMR (CDCl_3): 8.02 (d, $J = 2.3$ Hz, 1H), 7.75 (d, $J = 2.3$ Hz, 1H), 7.42 – 7.36 (m, 2H), 7.30 – 7.24 (m, 2H), 6.69 (d, $J = 8.5$ Hz, 1H), 6.59 (s, 1H), 6.28 – 6.22 (m, 1H), 6.03 (d, $J = 3.0$ Hz, 1H), 4.23 – 4.16 (m, 1H), 3.93 (s, 3H), 3.02 (dd, $J = 5.8, 14.9$ Hz, 1H), 2.95 – 2.88 (m, 2H), 2.79 (dd, $J = 8.2, 14.9$ Hz, 1H), 2.55 (dd, $J = 4.3, 17.1$ Hz, 1H), 1.13 – 1.01 (m, 2H), 0.95 – 0.88 (m, 1H), 0.56 – 0.48 (m, 1H). ^{13}C -NMR (CD_3OD): 178.3, 175.1, 164.7, 153.2, 147.5, 143.0, 141.2, 137.5, 137.1, 134.6, 133.1, 131.4, 131.3, 129.4, 111.5, 111.2, 108.3, 54.2, 40.6, 37.3, 31.7, 30.9, 7.9. HRMS: calcd 538.1204, found 538.1193, $\text{C}_{27}\text{H}_{25}\text{ClN}_3\text{O}_5\text{S}$.

4.9. (*R*)-3-(Cyclopentylmethyl)-4-(cyclopropyl(4-(2-(6-methoxy-pyridin-3-yl)phenyl)thiazol-2-yl)amino)-4-oxobutanoic acid (**10**) Using acid **42** (11.5 g, 45 mmol) and aminothiazole **50** (15.95 g, 49 mmol) amide bond formation step was carried out as per compd **1** except at 60 °C to obtain *tert*-butyl (*R*)-3-(cyclopentylmethyl)-4-(cyclopropyl(4-(2-(6-methoxy-pyridin-3-yl)phenyl)thiazol-2-yl)amino)-4-oxobutanoate (**57**) as a beige solid (14.2 g, 56%) after flash chromatography (10% EtOAc in cyclohexane). LCMS (Method B) m/z 562 ($M + 1$). HPLC purity > 98% (254 nm). ^1H NMR (300 MHz, CDCl_3): 8.08 (d, $J = 1.8$ Hz, 1H), 7.71 (d, $J = 6.9$ Hz, 1H), 7.40 – 7.38 (m, 4H), 6.65 (d, $J = 6.3$ Hz, 1H), 6.59 (s, 1H), 3.92 (s, 3H), 3.92 - 3.87 (m, 1H), 3.03 – 2.96 (m, 1H), 2.74 – 2.70 (m, 1H), 2.53 – 2.44 (m, 1H), 1.77 – 1.41 (m, 10H), 1.38 (s, 9H), 1.19 - 1.07 (m, 4H), 0.58 – 0.49 (m, 1H). Elemental analysis: calcd C, 68.42; H, 7.00; N, 7.48; found C, 68.27; H, 7.11; N, 7.25. **57** (14.3 g, 25 mmol) after TFA deprotection, as described for **1**, afforded **10** as white solid (10.9 g, 86%). LCMS (Method A) m/z 506 ($M + 1$). HPLC purity 96% (254 nm). ^1H NMR (CDCl_3): 8.08 (d, $J = 2.3$ Hz, 1H), 7.74 – 7.71 (m, 1H),

7.45 – 7.36 (m, 4H), 6.69 (d, $J = 8.6$ Hz, 1H), 6.63 (s, 1H), 3.94 (s, 3H), 3.88 – 3.81 (m, 1H), 3.05-2.99 (m, 1H), 2.91 (dd, $J = 9.4, 17.7$ Hz, 1H), 2.60 (dd, $J = 4.2, 17.5$ Hz, 1H), 1.87 – 1.75 (m, 3H), 11.64 – 1.45 (m, 7H), 1.14 – 0.95 (m, 5H), 0.60 – 0.53 (m, 1H). ^{13}C NMR (CD_3OD): 179.5, 179.2, 175.7, 164.5, 147.5, 141.4, 138.5, 132.5, 131.7, 131.6, 129.7, 128.9, 111.0, 106.3, 54.3, 42.1, 39.9, 39.6, 39.1, 36.8, 34.3, 33.7, 33.3, 31.7, 30.9, 26.0, 25.9, 7.8. HRMS: calcd 506.2113, found 506.2106, $\text{C}_{28}\text{H}_{32}\text{N}_3\text{O}_4\text{S}$. Elemental analysis: calcd C, 66.51; H, 6.18; N, 8.31; found C, 66.15; H, 6.12; N, 7.95.

4.10. (*R*)-4-((4-(2-(6-(1*H*-Pyrazol-1-yl)pyridin-3-yl)phenyl)thiazol-2-yl)(cyclopropyl)amino)-3-(cyclopentylmethyl)-4-oxobutanoic acid (**11**). Using acid **42** (0.51 g, 2 mmol) and aminothiazole **53** (200 mg, 0.56 mmol) amide bond formation step was carried out as per compd **1** except at 60 °C to obtain *tert*-butyl (*R*)-4-((4-(2-(6-(1*H*-pyrazol-1-yl)pyridin-3-yl)phenyl)thiazol-2-yl)(cyclopropyl)amino)-3-(cyclopentylmethyl)-4-oxobutanoate (**58**) as white solid (188 mg, 57%) after flash chromatography (10% EtOAc in cyclohexane). LCMS (Method B) m/z 598 ($M + 1$). HPLC purity > 98% (254 nm). **58** (188 mg, 0.31 mmol) after TFA deprotection, as described for **1**, afforded **11** as white solid (46 mg, 27%). LCMS (Method A) m/z 542 ($M + 1$). HPLC purity 95% (254 nm). ^1H NMR (CDCl_3): 8.50 (d, $J = 1.9$ Hz, 1H), 8.32 (d, $J = 1.7$ Hz, 1H), 7.84 (d, $J = 8.4$ Hz, 1H), 7.76 – 7.72 (m, 2H), 7.62 (dd, $J = 2.0, 8.6$ Hz, 1H), 7.49 – 7.39 (m, 3H), 6.72 (s, 1H), 6.49 – 6.45 (m, 1H), 3.88 – 3.79 (m, 1H), 2.86 – 2.76 (m, 2H), 2.60 (dd, $J = 4.0, 17.4$ Hz, 1H), 1.83 – 1.69 (m, 3H), 1.63 – 1.45 (m, 6H), 1.13 – 1.02 (m, 2H), 0.97 – 0.92 (m, 2H), 0.84 – 0.76 (m, 1H), 0.62 – 0.55 (m, 1H). ^{13}C NMR (CD_3OD): 179.5, 175.9, 162.0, 151.2, 149.3, 143.3, 140.9, 137.9, 137.4, 135.9, 131.7, 131.6, 129.8, 129.4, 128.3, 112.8, 109.0, 40.1, 39.9, 38.8, 37.0, 34.2, 33.3, 31.1, 26.0, 25.9, 7.8. HRMS: calcd 542.2226, found 542.2231, $\text{C}_{30}\text{H}_{32}\text{N}_5\text{O}_3\text{S}$.

4.11. (*R*)-3-(Cyclopropyl(4-(2-(6-methoxypyridin-3-yl)phenyl)thiazol-2-yl)carbamoyl)-5-methylhexanoic acid (**12**). Using acid **44** (640 mg, 2.78 mmol) and aminothiazole **50** (990 mg, 3.06 mmol) amide bond formation step was carried out as per compd **1** except at 60 °C to obtain *tert*-butyl (*R*)-3-(cyclopropyl(4-(2-(6-methoxypyridin-3-yl)phenyl)thiazol-2-yl)carbamoyl)-5-methylhexanoate (**59**) as white solid (751 mg, 1.40 mmol, 50%) after flash chromatography (10% EtOAc in cyclohexane). LCMS (Method B) m/z 536 ($M + 1$). HPLC purity > 98% (254 nm). **59** (751 mg, 1.40 mmol) after TFA deprotection, as described for **1**, afforded **12** as white solid (496 mg, 1.03 mmol, 74%). LCMS (Method A) m/z 480 ($M + 1$). HPLC purity 99% (254 nm). ^1H NMR (CDCl_3): 8.09 (d, $J = 2.3$ Hz, 1H), 7.74 – 7.71 (m, 1H), 7.44 – 7.40 (m, 3H), 7.36 – 7.33 (m, 1H), 6.69 (d, $J = 8.5$ Hz, 1H), 6.63 (s, 1H), 3.94 (s, 3H), 3.92 – 3.82 (m, 1H), 3.04 – 2.98 (m, 1H), 2.89 (dd, $J = 9.8, 17.2$ Hz, 1H), 2.56 (dd, $J = 4.1, 17.2$ Hz, 1H), 1.67 – 1.56 (m, 1H), 1.47 – 1.39 (m, 2H), 1.09 – 0.98 (m, 3H), 0.91 (d, $J = 17.4$ Hz, 6H), 0.60 – 0.54 (m, 1H). ^{13}C NMR (CD_3OD): 179.7, 175.9, 164.6, 162.3, 147.5, 141.3, 138.6, 135.8, 132.5, 131.7, 131.6, 129.7, 128.9, 111.0, 54.2, 42.6, 38.9, 36.8, 31.0, 26.8, 23.8, 22.1, 7.8. HRMS: calcd 480.1957, found 480.1953, $\text{C}_{26}\text{H}_{30}\text{N}_3\text{O}_4\text{S}$.

4.12. (*R*)-3-((4-(2-(6-(1*H*-Pyrazol-1-yl)pyridin-3-yl)phenyl)thiazol-2-yl)(cyclopropyl)carbamoyl)-5-methylhexanoic acid (**13**). Using acid **44** (640 mg, 2.78 mmol) and aminothiazole **53** (600 mg, 1.67 mmol) amide bond formation step was carried out as per compd **1** except at 60 °C to obtain *tert*-butyl (*R*)-3-((4-(2-(6-(1*H*-pyrazol-1-yl)pyridin-3-yl)phenyl)thiazol-2-yl)(cyclopropyl)carbamoyl)-5-methylhexanoate (**60**) as white solid (288 mg, 30%) after flash chromatography (10% EtOAc in cyclohexane). LCMS (Method A) m/z 572 ($M + 1$). HPLC purity > 98% (254 nm). ^1H NMR (CDCl_3): 8.54 (d, $J = 2.5$ Hz, 1H), 8.30 (d, $J = 2.1$ Hz, 1H), 7.92 (d, $J = 8.4$ Hz, 1H), 7.78 – 7.68 (m, 3H), 7.48 – 7.38 (m, 3H), 6.67 (s, 1H), 6.47 (t, $J = 2.1$

Hz, 1H), 3.91 – 3.85 (m, 1H), 2.99 – 2.95 (m, 1H), 2.73 (dd, $J = 9.3, 16.6$ Hz, 1H), 2.43 (dd, $J = 4.9, 16.6$ Hz, 1H), 1.63 – 1.53 (m, 2H), 1.39 (s, 9H), 1.10 - 0.94 (m, 3H), 0.89 (d, $J = 6.56$ Hz, 6H), 0.58 – 0.51 (m, 2H). **60** (288 mg, 0.50 mmol) after TFA deprotection, as described for **1**, afforded **13** as light yellow solid (242 mg, 93%). LCMS (Method A) m/z 516 ($M + 1$). HPLC purity 97% (254 nm). ^1H NMR (CDCl_3): 8.50 (d, $J = 2.4$ Hz, 1H), 8.37 (d, $J = 2.1$ Hz, 1H), 7.79 – 7.76 (m, 2H), 7.73 – 7.68 (m, 1H), 7.53 – 7.42 (m, 4H), 6.82 (s, 1H), 6.49 (dd, $J = 2.1, 2.4$ Hz, 1H), 3.92 - 3.82 (m, 1H), 2.87 – 2.76 (m, 2H), 2.55 (dd, $J = 3.7, 16.7$ Hz, 1H), 1.67 – 1.58 (m, 1H), 1.50 – 1.38 (m, 2H), 0.97 – 0.76 (m, 9H), 0.62 – 0.55 (m, 1H). ^{13}C NMR (CD_3OD): 179.7, 175.6, 151.2, 149.3, 143.3, 140.9, 138.0, 137.5, 135.9, 131.7, 131.6, 129.8, 129.5, 128.4, 112.8, 109.0, 42.6, 38.8, 36.6, 31.0, 26.7, 23.8, 22.1, 7.7. HRMS: calcd 516.2069, found 516.2077, $\text{C}_{28}\text{H}_{30}\text{N}_5\text{O}_3\text{S}$.

4.13. (R)-2-benzyl-4-(tert-butoxy)-4-oxobutanoic acid (17). The title compd was prepared following Scheme 1 (steps a-c). *Step a:* To a stirred solution of 4-(*tert*-butyl)-1-methyl-2-(dimethoxyphosphoryl)succinate (**14**, Scheme 1) (77 g, 0.26 mol) in THF (1 L), was added *n*-BuLi (1.6M in hexanes, 179 mL, 0.29 mol) dropwise (45 min) at 5-15°C (ice bath). The orange solution thus obtained was stirred at 5-15°C for 90 min. whereupon a THF solution (200 mL) of benzaldehyde (27.5 g, 0.26 mol) added dropwise (30 min) at 5-10°C. The viscous solution was then allowed to warm gradually to rt and stirred overnight. Thereafter the reaction was quenched with ice/water (300 mL), the volatiles removed in vacuo and the resultant residue taken up in saturated aq NaHCO_3 (400 mL) and then extracted with EtOAc (2 x 400 mL). The combined organic layers were dried over Na_2SO_4 and evaporated in vacuo to obtain a brown oil (85 g) that was purified by silica gel flash chromatography using an increasing gradient from 1-10% EtOAc /petroleum ether to obtain 4-(*tert*-butyl) 1-methyl (*E*)-2-benzylidenesuccinate **15** (31

g, 0.11 mol, 42%) as an off-white solid. LCMS (Method B) m/z 277 ($M + 1$). HPLC purity > 98% (254 nm). $^1\text{H NMR}$ (CDCl_3): 7.83 (s, 1H), 7.34 (m, 5H), 3.80 (s, 3H), 3.44 (s, 2H), 1.44 (s, 9H). *Step b*: To a stirred solution of **15** (29 g, 0.11 mol) in THF (600 mL) was added Bu_4NOH (1M in water, 210 mL, 0.21 mol) and stirred 75 minutes (reaction completion confirmed by LCMS). After removal of volatiles in vacuo, the reaction mixture was adjusted to pH 7 using pre-cooled 1M HCl (130 mL) and the cloudy suspension extracted with EtOAc (400 mL), washed with 0.5M HCl (3 x 200 mL), brine (50 mL) and dried (Na_2SO_4) to obtain (*E*)-2-benzylidene-4-(*tert*-butoxy)-4-oxobutanoic acid, **16** (21.4 g, 74%) as a pale yellow solid after removal of volatiles. LCMS (Method B) m/z 263 ($M + 1$). HPLC purity > 98% (254 nm). $^1\text{H NMR}$ (CDCl_3): 7.95 (s, 1H), 7.37 (m, 5H), 3.46 (s, 2H), 1.45 (s, 9H). *Step c*: To a solution of **16** (36 g, 0.137 mol) in methanol (270 mL) was added 27.36 mL (0.137 mol) of dicyclohexylamine whereupon the reaction vessel and mixture was thoroughly degassed using Ar. To this degassed solution was added $\text{RuCl}_2[(S)\text{-BINAP}]$ (350 mg, 0.4 mmol) under Ar and subsequently the reaction vessel was evacuated and back-filled with hydrogen three times; the hydrogen pressure was ultimately adjusted to 10 bars and reaction mixture heated (autoclave) at 55 °C and left stirring for 3 days whereupon the mixture was allowed to reach rt, degassed and concentrated to dryness to obtain the crude product (%ee 82.8). This crude dicyclohexylamine salt was recrystallized three times from $\text{CH}_3\text{CN}/\text{H}_2\text{O}$ (v/v, 50:1) and subsequently free-based by stirring the recrystallized salt in water, acidifying to pH 1 (6M aq. HCl) and EtOAc extraction to obtain **17** (17.3 g, 48%). LCMS (Method B) m/z 265 ($M + 1$). HPLC purity > 98% (254 nm). Chiral LC (Method C): > 98 %ee ($t_{\text{R}(R)}$ = 8.13 min, $t_{\text{R}(S)}$ = 8.97 min). $^1\text{H NMR}$ (CDCl_3): 7.34 (m, 5H), 3.1 (m, 2H), 2.76 (dd, J = 15.4, 10.6 Hz, 1H), 2.52 (dd, J = 16.8, 8.7 Hz, 1H), 2.36 (dd, J = 16.8, 4.2 Hz, 1H), 1.41 (s, 9H).

4.14. (*S*)-2-benzyl-4-(*tert*-butoxy)-4-oxobutanoic acid (**18**). To a solution of (*S*)-3-benzyl-4-methoxy-4-oxobutanoic acid (0.5 g, 2.25 mmol) and *tert*-butyl-2,2,2-trichloroacetimidate (0.8 mL, 4.51 mmol) in anhydrous THF (4 mL) under Ar at 0 °C was added BF₃·OEt₂ (42 μL, 0.34 mmol) dropwise. The reaction mixture was stirred for 1 h at 0 °C. Since conversion was incomplete (LCMS), additional *tert*-butyl-2,2,2-trichloroacetimidate (0.8 mL, 4.51 mmol) was added and mixture stirred for a further hour at 0 °C. Saturated NaHCO₃ (5 mL) was carefully added and mixture extracted with EtOAc (2x 10 mL). The combined organic layer was dried over MgSO₄, filtered and concentrated to dryness. The residue was then purified by flash chromatography on silica gel (5% EtOAc in cyclohexane) providing 4-(*tert*-butyl)-1-methyl-(*S*)-2-benzylsuccinate (0.54 g, 87%). LCMS (Method B) m/z 223 (M + 1 - *t*Bu). HPLC purity > 95% (254 nm). ¹H-NMR (CDCl₃) : 7.41 – 7.01 (m, 5H), 3.66 (s, 3H), 3.20 – 2.90 (m, 2H), 2.73 (m, 1H), 2.60 (dd, *J* = 16.5, 9.1 Hz, 1H), 2.33 (dd, *J* = 16.5, 4.7 Hz, 1H), 1.41 (s, 9H). To a solution of 4-(*tert*-butyl)-1-methyl-(*S*)-2-benzylsuccinate (0.54 g, 1.93 mmol) in THF/water (1/1, 8 mL) was added LiOH (185 mg, 7.73 mmol) and the reaction mixture stirred at rt for 14 h whereupon HCl (3 M) was added to adjust pH to 1. Thereafter, the mixture was extracted with DCM (3x 10 mL) and the combined extracts dried (MgSO₄), filtered and concentrated to dryness. The crude residue was purified by flash chromatography (40% EtOAc in cyclohexane) providing (*S*)-2-benzyl-4-(*tert*-butoxy)-4-oxobutanoic acid (**18**) (0.43 g, 85%). LCMS (Method B) m/z 209 (M + 1 - *t*Bu). HPLC purity > 98% (254 nm). ¹H-NMR (CDCl₃) : 10.49 (bs, 1H), 7.38 – 7.24 (m, 5H), 3.20 – 3.13 (m, 2H), 2.83 (dd, *J* = 15.4, 10.4 Hz, 1H), 2.62 (dd, *J* = 16.6, 8.6 Hz, 1H), 2.41 (dd, *J* = 16.6, 4.6 Hz, 1H), 1.48 (s, 9H).

4.15. 4-(2-Chlorophenyl)-*N*-methylthiazol-2-amine (**23**). *N*-methyl thiourea **19** (22 g, 0.24 mol) was added to a solution of 2-bromo-2'-chloroacetophenone **21** (64.5 g, 0.23 mol) in ethanol

(0.2M) and the reaction mixture heated to reflux for an hour whereupon the volatiles were removed and the resultant oil taken up in EtOAc/DCM (v/v, 1:1). The DCM was then evaporated and the suspension stirred overnight and the precipitate filtered and washed with EtOAc. The crude HBr salt was then free-based after being taken up in DCM/saturated NaHCO₃ solution (1:1), followed by drying of the extracted organic phase over Na₂SO₄ and removal of the volatiles to furnish **23** as a bright yellow solid (37.2 g, 69%). LCMS (Method B) *m/z* 225 (M + 1). HPLC purity > 98% (254 nm) ¹H NMR (CDCl₃) 7.84 (dd, *J* = 7.7, 1.9 Hz, 1H), 7.43 (dd, *J* = 7.8, 1.5 Hz, 1H), 7.36 - 7.13 (m, 3H), 7.00 (s, 1H), 5.69 (s, 1H), 2.96 (d, *J* = 3.7 Hz, 3H).

4.16. 4-(2-Chlorophenyl)-*N*-cyclopropylthiazol-2-amine (**24**). The title compd was prepared as per the procedure for **23** by using *N*-cyclopropyl thiourea **20** (200 mg, 1.7 mmol) and 2-bromo-2-chloroacetophenone **21** (402 mg, 1.7 mmol) to furnish **24** as a white solid (260 mg, 60%). LCMS (Method B) *m/z* 251 (M + 1). HPLC purity > 98% (254 nm). ¹H NMR (CDCl₃) 7.80 (dd, *J* = 7.6, 1.6 Hz, 1H), 7.48 – 7.36 (m, 1H), 7.29 – 7.17 (m, 2H), 6.14 (s, 1H), 2.59 (dt, *J* = 6.3, 3.2 Hz, 1H), 0.75 (q, *J* = 6.4, 5.9 Hz, 2H), 0.64 (q, *J* = 4.2 Hz, 2H).

4.17. *N*-cyclopropyl-4-(2,5-dichlorophenyl)thiazol-2-amine (**25**) The title compd was prepared as per the procedure for **23** by using *N*-cyclopropyl thiourea **20** (407 mg, 3.5 mmol) and 2-bromo-2,5-dichloroacetophenone **22** (937 mg, 3.5 mmol) to yield **25** as a yellow solid (940 mg, 94%). LCMS (Method B) *m/z* 286 (M + 1). HPLC purity > 98% (254 nm). ¹H NMR (CDCl₃) 7.87 (d, *J* = 2.6 Hz, 1H), 7.35 (d, *J* = 8.5 Hz, 1H), 7.20 (d, *J* = 2.6 Hz, 1H), 7.13 (s, 1H), 6.14 (s, 1H), 2.62 (tt, *J* = 6.7, 3.2 Hz, 1H), 0.84 – 0.75 (m, 2H), 0.68 (q, *J* = 3.2, 2.3 Hz, 2H).

4.18. (*R*)-4-(*Tert*-butoxy)-2-(cyclopentylmethyl)-4-oxobutanoic acid (**42**). The title compd was prepared as per Scheme 2 (steps a-d). *Steps a-b*: To a solution of 3-cyclopentylpropanoic acid **30** (46.6 g, 0.33 mol) in freshly distilled anhydrous THF (0.9 M) was added triethylamine (52 mL,

0.38 mol), the mixture was cooled to $-78\text{ }^{\circ}\text{C}$ and pivaloyl chloride (41 mL, 0.33 mol) was added dropwise, stirred for 15 min at $-78\text{ }^{\circ}\text{C}$ then allowed to warm to rt and stirred for 1 h (white suspension forms). To a solution of (*S*)-4-benzyloxazolidin-2-one (59.2 mg, 0.33 mol) in freshly distilled THF was added nBuLi (2.5 M in THF, 134 mL, 0.33 mol) and the mixture stirred for 20 min at $-78\text{ }^{\circ}\text{C}$ whereupon it was added to the pre-cooled ($-78\text{ }^{\circ}\text{C}$) pivalic anhydride prepared in situ above. The resultant mixture was stirred for 30 min at $-78\text{ }^{\circ}\text{C}$ whereupon the reaction was allowed to reach rt by removing the cooling bath. Saturated aq NH_4Cl (500 mL) was then added and the aq phase extracted with EtOAc (2 x 200 mL). Combined organic extracts were dried (MgSO_4), filtered and concentrated in vacuo. The crude thus obtained was subjected to flash chromatographic purification using 20% EtOAc in petroleum ether to obtain 91 g (91%) (*S*)-4-benzyl-3-(3-cyclopentylpropanoyl)oxazolidin-2-one (**34**) as white solid. $^1\text{H NMR}$ (CDCl_3) : 7.43 – 7.12 (m, 5H), 4.67 (ddt, $J = 10.2, 7.0, 3.4$ Hz, 1H), 4.27 – 4.10 (m, 2H), 3.30 (dd, $J = 13.4, 3.3$ Hz, 1H), 3.08 – 2.83 (m, 2H), 2.76 (dd, $J = 13.3, 9.6$ Hz, 1H), 1.93 – 1.42 (m, 10H), 1.20 – 1.04 (m, 2H). *Step c:* To a stirred solution of **34** (95 g, 0.315 mol) in THF (0.08 M) at $-78\text{ }^{\circ}\text{C}$ was added NaHMDS (1M in THF, 410 mL, 0.41 mol) dropwise over 1 h, whereupon *tert*-butyl bromoacetate (70 mL, 0.41 mol) was added dropwise over 30 min at $-78\text{ }^{\circ}\text{C}$. The cooling bath was then removed to allow the reaction to warm to rt and stirred overnight. The mixture was then cooled using an ice-bath and saturated aq NH_4Cl added slowly (300 mL), followed by water (100 mL); then the aq phase was extracted with EtOAc (200 mL) and the combined organic extracts dried (Na_2SO_4), filtered and evaporated to dryness. The thus obtained crude was purified by flash chromatography using 5-30% EtOAc in petroleum ether gradient to obtain 73 g (56%) of *tert*-butyl (*R*)-4-((*S*)-4-benzyl-2-oxooxazolidin-3-yl)-3-(cyclopentylmethyl)-4-oxobutanoate (**38**) as white solid. *Step d:* To a stirred solution of **38** (73 g, 0.18 mol) in 750 mL THF/water (4:1, v/v) at $0\text{ }^{\circ}\text{C}$ was added H_2O_2 (35% in water, 68 mL, 0.7

mol) dropwise over 15 min. Stirring was continued for 10 min, then 1M aq LiOH (300 mL, 0.35 mol) was added dropwise over 15 min whereupon the mixture was allowed to warm to rt and stirred for 16 h till reaction deemed completed by LCMS. The reaction mixture was cooled using an ice-bath and a solution of sodium bisulfite (225 g, 1.8 mol) in water (1 L) was added dropwise over 1 h. (Caution: slight exotherm during this addition!) The bulk of THF was removed in vacuo and the thus obtained aq layer (pH ~ 12) was washed with Et₂O (3x 500 mL), cooled (ice-bath) and acidified to pH 1-2 with 6M HCl and extracted with EtOAc (5x 500 mL). The combined extracts dried (MgSO₄), filtered and concentrated in vacuo to dryness to obtain the title compound, **42** (30 g, 65%) as pale yellow oil. ¹H NMR (CDCl₃) : 2.80 (td, *J* = 8.5, 7.6, 4.4 Hz, 1H), 2.60 (dd, *J* = 16.4, 9.3 Hz, 1H), 2.39 (dd, *J* = 16.4, 5.1 Hz, 1H), 1.96 – 1.65 (m, 5H), 1.49 (m, 4H), 1.43 (s, 9H), 1.07 (m, 2H).

4.19. (2*R*)-4-(*Tert*-butoxy)-4-oxo-2-((tetrahydro-2*H*-pyran-3-yl)methyl)butanoic acid (**43**).

Prepared as per Scheme 2 (steps a-d) detailed above for **42**. *Steps a-b*: 3-(tetrahydro-2*H*-pyran-4-yl)propanoic acid **31** (2.4g, 15.1 mmol) furnished after flash chromatography (40% EtOAc in petroleum ether) (*S*)-4-benzyl-3-(3-(tetrahydro-2*H*-pyran-4-yl)propanoyl)oxazolidin-2-one (**35**) as colorless oil (4 g, 84%). LCMS (Method B) *m/z* 318 (*M* + 1). HPLC purity 98% (254 nm). ¹H-NMR (CDCl₃) : 7.41 – 7.15 (m, 5H), 4.66 (ddt, *J* = 10.2, 6.8, 3.3 Hz, 1H), 4.28 – 4.12 (m, 2H), 3.88 (d, *J* = 12.1 Hz, 2H), 3.49 – 3.19 (m, 2H), 3.19 – 3.01 (m, 1H), 3.01 – 2.84 (m, 2H), 2.84 – 2.67 (m, 1H), 1.75 – 1.39 (m, 6H), 0.98 – 0.78 (m, 1H). *Step c*: **35** (4 g, 12.6 mmol) after flash chromatography (30% EtOAc in petroleum ether) furnished *tert*-butyl (3*R*)-4-((*S*)-4-benzyl-2-oxooxazolidin-3-yl)-4-oxo-3-((tetrahydro-2*H*-pyran-3-yl) methyl) butanoate (**39**) (3.26 g, 60%) as white solid LCMS (Method B) *m/z* 376 (*M* -56). HPLC purity 95% (254 nm). ¹H NMR (CDCl₃) : 7.35 – 7.25 (m, 5H), 4.70-4.63 (m, 1H), 4.33 – 4.28 (m, 2H), 4.19-4.17 (m, 2H), 3.98

– 3.91 (m, 2H), 3.39 – 3.30 (m, 3H), 2.82 – 2.7 (m, 2H), 2.53 – 2.46 (m, 1H), 1.71 – 1.58 (m, 5H), 1.44 (s, 9H). *Step d:* **39** (3.26 g, 7.5 mmol) furnished the title compd **43** (1.7 g, 83%) as a white solid. LCMS (Method B) m/z 217 ($M + 1 - tBu$). HPLC purity > 98% (254 nm). 1H NMR ($CDCl_3$) : 9.2 (bs, 1H), 3.98-3.94 (m, 2H), 3.41-3.34 (m, 2H), 2.99-2.84 (m, 1H), 2.77 (dd, $J = 17.0, 9.0$ Hz, 0.5H), 2.62 (dd, $J = 16.4, 9.0$ Hz, 0.5H), 2.50 (dd, $J = 17.0, 5.2$ Hz, 0.5H), 2.37 (dd, $J = 16.4, 5.2$ Hz, 0.5H), 1.77-1.54 (m, 4H), 1.42-1.23 (m, 3H), 1.43 (s, 9H).

4.20. (*R*)-2-(2-(*Tert*-butoxy)-2-oxoethyl)-4-methylpentanoic acid (**44**). Prepared as per Scheme 2 (steps a-d) detailed above for **42**. *Steps a-b:* 4-methylpentanoic acid **32** (3 g, 25.8 mmol) furnished (*S*)-4-benzyl-3-(4-methylpentanoyl)oxazolidin-2-one (**36**) as colorless oil (6.1 g, 86%). LCMS (Method B) m/z 276 ($M + 1$). HPLC purity 98% (254 nm). 1H NMR ($CDCl_3$) : 7.38 – 7.17 (m, 6H), 4.67 (dq, $J = 10.3, 3.5$ Hz, 1H), 4.24 – 4.10 (m, 2H), 3.30 (dd, $J = 13.3, 3.2$ Hz, 1H), 2.93 (dt, $J = 16.9, 8.6$ Hz, 2H), 2.76 (dd, $J = 13.3, 9.6$ Hz, 1H), 1.72 – 1.47 (m, 4H), 0.95 (d, $J = 6.2$ Hz, 6H). *Step c:* **36** (6.1 g, 22.15 mmol) furnished *tert*-butyl (*R*)-3-((*S*)-4-benzyl-2-oxooxazolidine-3-carbonyl)-5-methylhexanoate (**40**) (6.3 g, 16.18 mmol, 73% yield) as white solid. 1H -NMR ($CDCl_3$) : 7.39 – 7.18 (m, 6H), 4.72 – 4.58 (m, 1H), 4.25 (dq, $J = 10.0, 5.2$ Hz, 1H), 4.16 (d, $J = 4.3$ Hz, 2H), 3.35 (dd, $J = 13.5, 3.2$ Hz, 1H), 2.80 – 2.68 (m, 2H), 2.49 (dd, $J = 16.6, 4.6$ Hz, 1H), 1.69 – 1.47 (m, 3H), 1.47 – 1.21 (m, 13H), 0.93 (t, $J = 5.8$ Hz, 6H). *Step d:* **40** (6.3 g, 16.1 mmol) furnished title compd **44** (3.4 g, 91%) as white solid. 1H NMR ($CDCl_3$) : 2.96 – 2.68 (m, 1H), 2.59 (dd, $J = 16.4, 9.3$ Hz, 1H), 2.37 (dd, $J = 16.4, 5.1$ Hz, 1H), 1.73 – 1.51 (m, 2H), 1.43 (s, 9H), 1.38 – 1.28 (m, 1H), 0.93 (ddd, $J = 9.6, 6.3, 2.8$ Hz, 6H).

4.21. (*R*)-4-(*Tert*-butoxy)-2-(furan-2-ylmethyl)-4-oxobutanoic acid (**45**). Prepared as per Scheme 2 (steps a-d) detailed above for **42**. *Steps a-b:* 3-(furan-2-yl)propanoic acid **33** (1 g, 7.14 mmol) furnished (*S*)-4-benzyl-3-(3-(furan-2-yl)propanoyl)oxazolidin-2-one (**37**) as pale yellow solid

(0.983 g, 46%). LCMS (Method B) m/z 300 ($M + 1$). HPLC purity 96% (254 nm). ^1H NMR (CDCl_3) : 7.36 – 7.27 (m, 4H), 7.21 - 7.18 (m, 2H), 6.29 (dd, $J = 3.0, 1.9$ Hz, 1H), 6.08 (dd, $J = 3.2, 0.7$ Hz, 1H), 4.71 - 4.66 (m, 1H), 4.24 – 4.15 (m, 2H), 3.32 – 3.21 (m, 3H), 3.06 (t, $J = 7.3$ Hz, 2H), 2.78 (dd, $J = 13.3, 9.5$ Hz, 1H). *Step c*: **37** (0.97 g, 2.91 mmol) furnished *tert*-butyl (*R*)-4-((*S*)-4-benzyl-2-oxooxazolidin-3-yl)-3-(furan-2-ylmethyl)-4-oxobutanoate (**41**) (0.84 g, 2.03 mmol, 70% yield) as white solid. LCMS (Method B) m/z 358 ($M + 1 - t\text{Bu}$). HPLC purity 95% (254 nm). *Step d*: **41** (0.84 mg, 2.0 mmol) furnished the title compd **45** (0.43mg, 83% yield) as colorless oil. LCMS (Method B) m/z 277 ($M + \text{Na}$). HPLC purity 97% (254 nm) ^1H -NMR (CDCl_3) : 7.32 (m, 1H), 6.28 (dd, $J = 3.2, 1.8$ Hz, 1H), 6.08 (d, $J = 3.2$ Hz, 1H), 3.24 – 3.07 (m, 2H), 2.91 (dd, $J = 14.7, 7.8$ Hz, 1H), 2.58 (dd, $J = 16.9, 8.4$ Hz, 1H), 2.43 (dd, $J = 16.9, 4.9$ Hz, 1H), 1.43 (s, 9H).

4.22. *N*-Cyclopropyl-4-(2-(6-methoxy-pyridin-3-yl)phenyl)thiazol-2-amine (**50**). The title compd was prepared as per Scheme 3 (steps a-b). *Step a*: To a solution of 2'-bromoacetophenone **46** (100 g, 0.50 mol), in THF (100 mL) at 0 °C was added AlCl_3 (3.37 g, 0.025 mol) followed by dropwise addition of Br_2 (28.3 mL, 0.552 mol) over 90 min. The mixture was then allowed to warm to rt and stirred for 2 h whereupon it was quenched by addition of water (500 mL) and extracted with EtOAc (3 x 300 mL). (Note: the first extract is denser than water due to concentration.) The combined organic layer washed with brine (2 x 400 mL), dried (MgSO_4), filtered and concentrated in vacuo to obtain 2-bromo-(2'-bromoacetophenone) as yellow oil (215.4 g) and was used as crude. The 2-bromo-(2'-bromoacetophenone) (176.9 g, 0.414 mol) thus obtained was dissolved in ethanol (1.8 L) and 1-cyclopropylthiourea **20** (48 g, 0.414 mol) and the mixture refluxed for 2 h then allowed to cool to rt and the mixture concentrated to 150 mL whereupon diethyl ether (2.2 L) was added with rapid stirring resulting in a precipitate that

was filtered and air-dried to obtain the HBr salt of the desired product (145 g). This salt was then suspended in DCM (1.1 L) and washed with saturated NaHCO₃ (2 x 900 mL) to free base the product. The organic layer was dried (Na₂SO₄), filtered and concentrated to obtain **48** as an off-white solid (101 g, 83%). LCMS (Method B) *m/z* 296 (M + 1). HPLC purity > 98% (254 nm). ¹H NMR (CDCl₃) : 7.69 – 7.62 (m, 2H), 7.35 – 7.29 (m, 1H), 7.19 – 7.11 (m, 1H), 6.91 (s, 1H), 6.56 (bs, 1H), 2.60 – 2.53 (m, 1H), 0.72 – 0.65 (m, 2H), 0.62 – 0.56 (m, 2H). *Step b*: A mixture of **48** (1 g, 3.39 mmol), aq 2M K₂CO₃ (5.1 mL, 10.2 mmol), 6-methoxyipyridine-3-boronic acid (1.04 g, 6.78 mmol) and toluene (30 mL) was degassed with Ar for 10 min. Pd₂(dba)₃ (0.31 g, 0.34 mol) and S-Phos (0.28 g, 0.68 mmol) were then added and the mixture heated to 85 °C for 90 min. After allowing the mixture to cool to rt the reaction mixture was diluted with EtOAc (100 mL) and washed with brine (50 mL). The aq layer was further extracted with EtOAc (2x 50 mL) and then the combined extracts dried (MgSO₄), filtered and concentrated in vacuo. The crude (brown viscous oil) was purified by flash chromatography using 20-50% EtOAc in cyclohexane to obtain **50** as yellow solid (0.99 g, 90%). LCMS (Method B) *m/z* 324 (M + 1). HPLC purity > 98% (254 nm). ¹H NMR (CDCl₃) : 7.73 (d, *J* = 2.6 Hz, 1H), 7.55 (d, *J* = 8.5 Hz, 1H), 7.12 (dd, *J* = 2.6, 8.5 Hz, 1H), 7.00 (bs, 1H), 2.59 – 2.55 (m, 1H), 0.74 – 0.69 (m, 2H), 0.63 – 0.59 (m, 2H).

4.23. *4-(5-Chloro-2-(6-methoxyipyridin-3-yl)phenyl)-N-cyclopropylthiazol-2-amine* (**51**).

Prepared as per Scheme 3 (steps a-b) detailed above for **50**. *Step a*: 2'-bromo-5'-chloroacetophenone **47** (4.43 g, 19.0 mmol) furnished **49** as a yellow solid (5.6 g, 89%). LCMS (Method B) *m/z* 330 (M + 1). HPLC purity > 98% (254 nm). ¹H NMR (CDCl₃) : 7.73 (d, *J* = 2.6 Hz, 1H), 7.55 (d, *J* = 8.5 Hz, 1H), 7.12 (dd, *J* = 2.6, 8.5 Hz, 1H), 7.00 (bs, 1H), 2.59 – 2.55 (m, 1H), 0.73 – 0.68 (m, 2H), 0.63 – 0.57 (m, 2H). *Step b*: **49** (0.5 g, 1.52 mmol) furnished the title

product **51** as a light brown solid (0.17 g, 31%). LCMS (Method B) m/z 358 ($M + 1$). HPLC purity > 98% (254 nm). $^1\text{H NMR}$ (CDCl_3) : 8.08 (d, $J = 2.4$ Hz, 1H), 7.75 (d, $J = 2.2$ Hz, 1H), 7.41 (dd, $J = 2.5, 8.5$ Hz, 1H), 7.33 (dd, $J = 2.2, 8.2$ Hz, 1H), 7.25 (d, $J = 8.2$ Hz, 1H), 6.70 (d, $J = 8.5$ Hz, 1H), 6.21 (bs, 1H), 5.90 (s, 1H), 3.96 (s, 1H), 2.59 – 2.51 (m, 1H), 0.74 – 0.69 (m, 2H), 0.62 – 0.58 (m, 2H).

4.24. 4-(2-(6-(1H-Pyrazol-1-yl)pyridin-3-yl)phenyl)-N-cyclopropylthiazol-2-amine (**53**). The title compd was prepared as per steps c and d in Scheme 3. *Step c*: To a stirred solution of **48** (3 g, 10.16 mmol) in freshly distilled THF (56 mL) under Ar at -78°C , $n\text{BuLi}$ (8.9 mL, 2.5 M in hexanes, 22.3 mmol) was added dropwise and stirred for 15 min, whereupon freshly distilled $\text{B}(\text{O}i\text{-Pr})_3$ (7.1 mL, 30.5 mmol) was added. The mixture was stirred for 1 h at -78°C , then allowed to warm to rt and stirred for an additional hour. The volatiles were then removed in vacuo obtain 3.4 g of crude product (green solid) as • 1:1 mixture (LCMS) of the desired (2-(2-(cyclopropylamino)thiazol-4-yl)phenyl)boronic acid (**52**) and the debrominated N-cyclopropyl-4-phenylthiazol-2-amine side-product. This product was used as crude in step d. *Step d*: A mixture of crude crude **52** (2.64 g, 5.1 mmol active based on 50% purity by LCMS) and 5-bromo-2-(1H-pyrazol-1-yl)pyridine (1.14 g, 5.08 mmol) K_2CO_3 (2M aq, 7.6 mL, 15.2 mmol) in toluene (50 mL) was degassed for 10 min with Ar, then $\text{Pd}(\text{PPh}_3)_4$ (0.59 g, 0.5 mmol) was added and the mixture was refluxed for 6 h. Thereafter the mixture was left to cool to rt, washed with sat. NaHCO_3 (25 mL) and extracted with DCM (2x 35 mL). The extracted organic residue was dried (MgSO_4), filtered and concentrated in vacuo to obtain the crude oil that was subjected to flash chromatography using 30% EtOAc in Pet. Ether to obtain the title product as a tan solid (1.8 g, 89%). LCMS (Method B) m/z 360 ($M + 1$). HPLC purity 90% (254 nm). $^1\text{H NMR}$ (CDCl_3) 8.59 – 8.55 (m, 1H), 8.39 – 8.31 (m, 1H), 7.96 – 7.91 (m, 1H), 7.76 – 7.69 (m, 3H),

7.44 – 7.35 (m, 3H), 6.55 (br, 1H), 6.50 – 6.46 (m, 1H), 5.98 (s, 1H), 2.52 – 2.47 (m, 1H), 0.66 - 0.62 (m, 2H), 0.55 – 0.51 (m, 2H).

Supplementary Material. Additional information on PK data, plasma protein binding and various pharmacology assays are provided.

Corresponding Author

*(H.R.H.) E-mail: hamidhoveyda@hotmail.com

ORCID

Hamid Hoveyda: 0000-0003-4073-3535

Present Addresses

† For D.S.: Galapagos NV, Gen. De Wittelaan L11 A3, 2800 Mechelen, Belgium

▪ For C.B.: AlzProtect, 70 rue de Dr Yersin, 59120 Loos, France

□ For J.B. : DIAFIR SA, Ave Chardonnet, 35000 Rennes, France

‡ For F.O.: Id Campus, 5 rue Lambert Lombard, 4000 Liège, Belgium

Funding

This work was supported in part by the Ministry of Sustainable Development and Public Works, Walloon Region, Belgium (at Ogeda) and by Digestive and Kidney Diseases grants (DK033651, DK074868, DK063491 and DK09062) to J. M. O.

Acknowledgments

We warmly thank our colleagues in the compound profiling team for conducting studies in support of the work herein as well as Dr Lisa Haigh (Imperial College, London, UK) for obtaining the HRMS data.

Abbreviations

AUC_u, unbound area-under-the-curve; (S)-BINAP, (S)-(-)-(1,1'-binaphthalene-2,2'-diyl)bis(diphenylphosphine); CL_u, unbound systemic clearance rate; Compd, compound; DIEA, *N,N*-diisopropyl ethylamine, EtOAc, ethyl acetate; FFA2 receptor, free fatty acid-2 receptor; Fsp³, fraction sp³ = number of sp³ hybridized carbons/total carbon count; GPCR, G-protein coupled receptor; GTP- $\gamma^{35}\text{S}$, guanosine 5'-O-[gamma-thio]triphosphate; KO, knock-out mice model; HATU, *N*-[(Dimethylamino)-1*H*-1,2,3-triazolo-[4,5-*b*]pyridin-1-ylmethylene]-*N*-methylmethanaminium hexafluorophosphate *N*-oxide; HTS, high-throughput screening, NMM, *N*-methyl morpholine; OGTT, oral glucose tolerance test; POC, proof-of-concept; PK, pharmacokinetics; SAR, structure-activity relationship; $T_{1/2}$, elimination half-life.

References and notes

(1) Le Poul, E.; Loison, C.; Struyf, S.; Springael, J.-Y.; Lannoy, V.; Decobecq, M.-E.; Brezillion, S.; Dupriez, V.; Vassart, G.; Van Damme, J.; Parmentier, M.; Dutheux, M. Functional characterization of human receptors for short chain fatty acids and their role in polymorphnuclear cell activation. *J. Biol. Chem.* **2003**, 278, 25481-25489.

(2) Brown, A. J.; Goldsworthy, S. M.; Barnes, A. A.; Eilert, M. M.; Tcheang, L., Daniels, D.; Muir, A. I.; Wigglesworth, M. J.; Kinghorn, I.; Fraser, N. J.; Pike, N. B.; Strum, J. C.; Steplewski, K. M.; Murdock, P. R.; Holder, J. C.; Marshall, F. H.; Szekeres, P. G.; Wilson, S.;

Ignar, D. M.; Foord, S. M.; Wise, A.; Dowell, S. J. The orphan G protein-coupled receptors GPR41 and GPR43 are activated by propionate and other short chain carboxylic acids. *J. Biol. Chem.* **2003**, *278*, 11312-11319.

(3) Hoveyda, H.; Brantis, C. E. ; Dutheil, G. ; Zoute, L. ; Schils, D. ; Bernard, J. Compounds, pharmaceutical composition and methods for use in treating metabolic disorders. PCT application WO066682, priority date: December 8, 2008, publication date: June 17, 2010.

(4) Brantis, C. E.; Ooms, F.; Bernard, J. Novel amino acid derivatives and their use as GPR43 modulators. PCT application WO092284, priority date: January 29, 2010, publication date: August 4, 2011.

(5) Milligan, G.; Shimpukade, B.; Ulven, T.; Hudson, B. D. Complex pharmacology of free fatty acid receptors. *Chem. Rev.* **2017**, *117*, 67–110. See sections 3.5.1 and 3.5.2.

(6) For example **8**, as well as our antagonist reference ligand **2** (ES227703),²¹ are cited as reference ligands for FFA2 receptor in IUPHAR/BPS Guide to Pharmacology; see: <http://www.guidetopharmacology.org/GRAC/FamilyDisplayForward?familyId=24>.

(7) Hong, Y.-H.; Nishimura, Y.; Hishikawa, D.; Tsuzuki, H.; Miyahara, H.; Gotoh, C.; Choi, K.-C.; Feng, D., D.; Chen, C.; Lee, H.-G.; Katoh, K.; Roh, S.-G.; Sasaki, S. Acetate and propionate short chain fatty acids stimulate adipogenesis via GPR43. *Endocrinology* **2005**, *146*, 5092-5099.

(8) Tolhurst, G.; Heffron, H.; Lam, Y. S.; Parker, H. E.; Habib, A. M.; Diakogiannaki, E.; Cameron, J.; Grosse, J.; Reimann, F.; Gribble, F. M. Short-chain fatty acids stimulate glucagon-like peptide-1 secretion via the G-protein-coupled receptor FFAR2. *Diabetes* **2012**, *61*, 364-371.

(9) Villa, S. R.; Priyadarshini, M.; Fuller, M. H. ; Bhardwaj, T. ; Brodsky, M. R.; Anguiera, A. R.; Mosser, R. E.; Carboneau, B. A.; Tersey, S. A.; Mancebo, H.; Gilchrist, A.; Mirmira, R.G.;

Gannon, M.; Layden, B. T. Loss of free fatty acid receptor 2 leads to impaired islet mass and beta cell survival. *Sci. Rep.* **2016**, *6*, 28159.

(10) Tang, C.; Ahmed K.; Gille A.; Lu S.; Gröne H.J.; Tunaru S.; Offermanns S. Loss of FFA2 and FFA3 increases insulin secretion and improves glucose tolerance in type 2 diabetes. *Nature Medicine* **2015**, *21*, 173-179

(11) Bjursell, M.; Admyre, T.; Göransson, M.; Marley, A. E.; Smith, D. M.; Oscarsson, J.; Bohlooly-Y, M. Improved glucose control and reduced body fat mass in free fatty acid receptor 2-deficient mice fed a high-fat diet. *Am. J. Physiol. Endocrinol. Metab.* **2010**, *300*, E211-E220.

(12) McNelis, J. C.; Lee, Y. S.; Mayoral, R.; van der Kant, R.; Johnson, A. M. F.; Wollam, J.; Olefsky, J. M. GPR43 potentiates β -cell function in obesity. *Diabetes* **2015**, *64*, 3203-3217.

(13) Kimura, I.; Ozawa, K.; Inoue, D.; Imamura, T.; Kimura, K.; Maeda, T.; Terasawa, K.; Kashihara, D.; Hirano, K.; Tani, T.; Takahashi, T.; Miyauchi, S.; Shioi, G.; Inoue, H.; Tsujimoto
The gut microbiota suppresses insulin-mediated fat accumulation via the short-chain fatty acid receptor GPR43 *Nat. Commun.*, **2013**, *4*, 1829.

(14) Nakajima, A.; Nakatani, A.; Hasegawa, S.; Irie, J.; Ozawa, K.; Tsujimoto, G.; Suganami, T.; Itoh, H.; Kimura, I. The short chain fatty acid receptor GPR43 regulates inflammatory signals in adipose tissue M2-type macrophages. *PLoS One*, **2017**, *12*, e0179696.

(15) Priyadarshini, M.; Villa, S.R.; Fuller, M.; Wicksteed, B.; Mackay, C.R.; Alquier, T.; Poitout, V.; Mancebo, H.; Mirmira, R.G.; Gilchrist, A.; Layden, B.T. An acetate-specific GPCR, FFAR2, regulates insulin secretion. *Mol. Endocrinol.*, **2015**, *29*, 1055-1066.

(16) Sina, S.; Gavrilova, O.; Förster, M.; Till, A.; Derer, S.; Hildebrand, F.; Raabe, B.; Chalaris, A.; Scheller, J.; Rehmann, A.; Franke, A.; Ott, S.; Häslner, R.; Nikolaus, S.; Fölsch, U. R.; Rose-John, S.; Jiang, H.-P.; Li, J.; Schreiber, S.; Rosenstiel, P. G protein-coupled receptor 43 is

essential for neutrophil recruitment during intestinal inflammation. *J. Immunol.* **2009**, *183*, 7514-7522.

(17) Maslowski, K. M.; Vieira, A. T.; Ng, A.; Kranich, J.; Sierro, F.; Yu, D.; Schilter, H. C.; Rolph, M. S.; Mackay, F.; Artis, D.; Xavier, R. J.; Teixeira, M. M.; Mackay, C. R. Regulation of inflammatory responses by gut microbiota and chemoattractant receptor GPR43. *Nature* **2009**, *461*, 1282-1287.

(18) Smith, P. M.; Howitt, M. R.; Panikov, N.; Michaud, M.; Gallini, C. A.; Bohlooly-Y., M.; Glickman, J. N.; Garrett, W. S. The microbial metabolites, short-chain fatty acids, regulate colonic T_{reg} cell homeostasis. *Science* **2013**, *341*, 569-573.

(19) GLPG0974, an antagonist to FFA2 receptor, was developed by Galapagos. Top-line results from a phase 2a trial indicated that there was “no measurable clinical difference between GLPG0974 treated patients and placebo within 4 weeks”; see: (a) Vermeire, S.; Kojecký, V.; Knoflíček, V.; Reinisch, W.; Van Kaem, T.; Namour, F.; Beets, J.; Vanhoute, F. In GLPG0974, an FFA2 antagonist, in ulcerative colitis: efficacy and safety in a multicenter proof-of-concept study (Abstract DOP030); 10th Congress of ECCO (European Crohn’s and Colitis Organisation), Barcelona, February 18-21, 2015, Abstract DOP030, p. S39. For medicinal chemistry development and phase 1 safety see the following reports: (b) Pizzonero, M.; Dupont, S.; Babel, M.; Beaumont, S.; Bienvenu, N.; Blanqué, R.; Cherel, L.; Christophe, T.; Crescenzi, B.; De Lemos, E.; Delerive, P.; Deprez, P.; De Vos, S.; Djata, F.; Fletcher, S.; Kopiejewski, S.; L’Ebraly, C.; Lefrançois, J.-M.; Lavazais, S.; Manioc, M.; Nelles, L.; Oste, L.; Polancec, D.; Quéhéhen, V.; Soulas, F.; Triballeau, N.; van der Aar, E. M.; Vandeghinste, N.; Wakselman, E.; Brys, R.; Saniere, L. Discovery and optimization of an azetidone chemical series as a free fatty acid receptor 2 (FFA2) antagonist: From Hit to Clinic. *J. Med. Chem.* **2014**, *57*, 10044–10057.

- (c) Namour, F.; Galien, R.; Van Kaem, T.; Van der Aa, A.; Vanhoutte, F.; Beetens, J.; van't Klooster, G. Safety, pharmacokinetics and pharmacodynamics of GLPG0974, a potent and selective FFA2 antagonist, in healthy male subjects. *Br. J. Clin. Pharmacol.* **2016**, *82*, 139–148.
- (20) Propionate $pEC_{50} = 3.59 \pm 0.19$, E_{max} set to 100% ($N = 10$), vs *h*FFA2 in CHO cells.
- (21) Fraser, G. L.; Rorive, S.; Bernard, J.; Ooms, F.; Dremier, S.; Brantis, C.; Hoveyda, H. R. Radioligand binding properties and pharmacological characterization of ES227703, a selective antagonist of the human FFA2 receptor; manuscript in preparation.
- (22) (a) Lee, T.; Schwandner, R.; Swaminath, G.; Weizmann, J.; Cardozo, M.; Greenberg, J.; Jaeckel, P.; Ge, H.; Wang, Y.; Jiao, X.; Liu, J.; Kayser, F.; Tian, H.; Li, Y. Identification and functional characterization of allosteric agonists for the G protein-coupled receptor FFA2. *Mol. Pharmacol.* **2008**, *74*, 1599-1609. (b) Wang, Y.; Jiao, X.; Kayser, F.; Liu, J.; Wang, Z.; Wanska, M.; Greenberg, J.; Weizmann, J.; Ge, H.; Tian, H.; Wong, S.; Schwandner, R.; Lee, T.; Li, Y. The first synthetic agonists of FFA2: Discovery and SAR of phenylacetamides as allosteric modulators. *Bioorg. Med. Chem. Lett.* **2010**, *20*, 493-498.
- (23) It is worth to note in passing that the presence of *N*-thiazolylamide in both the foregoing agonist scaffold as well as in the Amgen allosteric agonist **3** (Fig. 1) was fortuitous in that we were unaware of the existence of **3** until well after our discovery and first round lead optimization of the *N*-thiazolylamide carboxylic acid scaffold discussed herein.
- (24) (a) Waring, M. J.; Arrowsmith, J.; Leach, A. R.; Leeson, P. D.; Mandrell, S.; Owen, R. M.; Pairaudeau, G.; Pennie, W. D.; Pickett, S. D.; Wang, J.; Wallace, O.; Weir, A. An analysis of the attrition of drug candidates from four major pharmaceutical companies. *Nature Rev. Drug Discovery* **2015**, *14*, 475-486. (b) Gleeson, M. P.; Hersey, A.; Montanari, D.; Overington, J.

Probing the links between in vitro potency, ADMET and physicochemical parameters. *Nature Rev. Drug Discovery* **2011**, *11*, 197–208.

(25) (a) Leeson, P. D.; Springthorpe, B. The influence of drug-like concepts in decision-making in medicinal chemistry. *Nature Rev. Drug Discovery* **2007**, *6*, 881–890. (b) Hopkins, A. L.; Keserü, G. M.; Lesson, P. D.; Rees, D. C.; Reynolds, C. H. The role of ligand efficiency metrics in drug discovery. *Nature Rev. Drug Discovery* **2014**, *13*, 105–121.

(26) Gocan, S., Cimpan, G, Comer, J. Lipophilicity Measurements by Liquid Chromatography. In *Advances in Chromatography*, Vol. 44; Grushka, E., Grinberg, N., Eds.; CRC Press: Boca Raton, **2005**, pp 79–176.

(27) (a) Lovering, F.; Bikker, J.; Humblet, C. Escape from flatland: increasing saturation as an approach to improving clinical success. *J. Med. Chem.* **2009**, *52*, 6752–6756. (b) Luker, T.; Alcaraz, L.; Chohan, K. K.; Blomberg, N.; Brown, D. S.; Butlin, R. J.; Elebring, T.; Griffin, A. M.; Guile, S.; St-Gallay, S.; Swahn, B.-M.; Swallow, S.; Waring, M. J.; Wenlock, M. C.; Leeson, P. D. Strategies to improve in vivo toxicology outcomes for basic candidate drug molecules. *Bioorg. Med. Chem. Lett.* **2011**, *21*, 5673–5679.

(28) Hann, M. Molecular obesity, potency and other addictions in drug discovery. *MedChemComm* **2011**, *2*, 349–355.

(29) Ritchie, T. J.; Macdonald, S. J. F. The impact of aromatic ring count on compound developability – are too many aromatic rings a liability in drug design? *Drug Discovery Today* **2009**, *14*, 1011–1019.

(30) Morphy, R. The influence of target family and functional activity on the physicochemical properties of pre-clinical compounds. *J. Med. Chem.* **2006**, *49*, 2969-2978.

(31) Hudson, B. D.; Tikhonova, I. G.; Pandey, S. K.; Ulven, T.; Milligan, G. Extracellular ionic locks determine variation in constitutive activity and ligand potency between species orthologs of the free fatty acid receptors FFA2 and FFA3. *J. Biol. Chem.* **2012**, *287*, 41195-41209.

(32) Sergeev, E., Hansen, A. H.; Pandey, S. K.; Mackenzie, A. E.; Hudson, B. D.; Ulven, T.; Milligan, G. Non-equivalence of key positively charged residues of the Free Fatty Acid 2 receptor in the recognition and function of agonist versus antagonist ligands. *J. Biol. Chem.* **2016**, *291*, 303-317.

(33) In contrast to other researchers who have used **8** extensively to explore various aspects of the FFA2 receptor pharmacology; e.g.: Hudson, B. D.; Due-Hansen, M. E.; Christiansen, E.; Hansen, A. M.; Mackenzie, A. E.; Murdoch, H.; Pandey, S. K.; Ward, R. J.; Marquez, R.; Tikhonova, I. G.; Ulven, T.; Milligan, G. Defining the molecular basis for the first potent and selective orthosteric agonists of the FFA2 free fatty acid receptor. *J. Biol. Chem.* **2013**, *288*, 17296-17312.

(34) To be noted, Brown et al have recently reported that the initial lead **1** from the foregoing scaffold as well as Amgen's allosteric agonist **3** are active in ex vivo lipolysis assays in murine adipocyte tissue explants from wild-type mice (at 75 μ M, 1% BSA), but not from FFA2 knock-out mice, as evidence that the ex-vivo lipolysis effect is FFA2 mediated; see: Brown, A. J.; Tsoulou, C.; Ward, E.; Gower, E.; Bhudia, N.; Chowdhury, F.; Dean, T. W.; Faucher, N.; Gangar, A.; Dowell, S. J. Pharmacological properties of acid N-thiazolylamide FFA2 agonists. *Pharma Res. Per.* **2015**, e00141, 1-15. However, in repeat testing, we have found that in mice **1** is inactive in both in vivo lipolysis and in OGTT assays despite its acceptable PK profile (C_{max} = 300 μ M, 30 mg/kg oral dose). In addition, Hudson et al. (ref. 31) have reported that the early generation lead **8** exhibits inhibitory effect in ex vivo lipolysis assays using human and murine

cell lines. Here again the effect was not demonstrated in vivo and nor was the mode-of-action verified through knock-out mice.

(35) Compound **13** is the best lead structure herein due to its superior in vivo oral exposure (Table 2) in step with its improved physicochemical properties (Table 1) when compared to **10**. Analogue **10** was used for the mechanism-of-action studies as this lead was discovered earlier and was deemed adequate for these studies.

(36) Due-Hansen et al advocate in situ acyl fluoride activation at 80 °C for more efficient coupling between *N*-cyclopropylthiazolamine (**24-25**, Scheme 1) and carboxylic acid **17** (racemate used in their work) versus HATU/DIEA amide coupling at ambient temperature. We obtain comparable yields with HATU/DIEA coupling at 60 °C, as also noted in our initial patent (see ref 3 above). Due-Hansen, M. E.; Pandey, S. K.; Christiansen, E.; Andersen, R.; Hansen, S. V. F.; Ulven, T. A protocol for amide bond formation with electron deficient amines and sterically hindered substrates. *Org. Biomol. Chem.* **2016**, *14*, 430-433.

(37) (a) Hoveyda, H.; Schils, D.; Zoute, L.; Parcq, J. Pyrrolidine or thiazolidine carboxylic acid derivatives, pharmaceutical composition and methods for use in treating metabolic disorders as agonists of G-protein coupled receptor 43 (GPR43). PCT application WO073376, priority date: December 18, 2009, publication date: June 23, 2011. (b) Hoveyda, H.; Schils, D.; Zoute, L.; Parcq, J.; Bernard, J.; Fraser, G. Compounds, pharmaceutical composition and method for use in treating inflammatory diseases. PCT application WO078949, priority date: November 27, 2013, publication date: June 4, 2015.

Graphical Abstract

***N*-Thiazolylamide-based free fatty-acid 2
receptor agonists: Discovery, lead
optimization and demonstration of off-target
effect in a diabetes model**

Hamid R. Hoveyda,^{a,*} Graeme L. Fraser,^a Ludivine Zoute,^a Guillaume Dutheuil,^a Didier Schils,^a Cyrille Brantis,^a Alexey Lapin,^a Julien Parcq,^a Sandra Guitard,^a François Lenoir,^a Mohamed El Bousmaqui,^a Sarah Rorive,^a Sandrine Hospied,^a Sébastien Blanc,^a Jérôme Bernard,^a Frédéric Ooms,^a Joanne C. McNelis^b and Jerrold M. Olefsky^b

^a Ogeda SA (formerly Euroscreen), 47 rue Adrienne Bolland, 6041 Gosselies, Belgium

^b University of California, ^aDepartment of Medicine, San Diego, La Jolla, USA

